Journal of Paleolimnology **11**: 41–65, 1994.

Sedimentary facies, depositional processes and climatic controls in a Triassic Lake, Tanzhuang Formation, western Henan Province, China *

María Gabriela Mángano[1], Luis Alberto Buatois[1], Xiantao Wu[2], Junmin Sun[2] & Guocheng Zhang[2]
[1] *Facultad de Ciencias Naturales, Universidad Nacional de Tucumán, Casilla de correo 1 (CC), 4000 San Miguel de Tucumán, Argentina*
[2] *Jiaozuo Mining Institute, Jiaozuo City, Henan Province, P.R. China*

Received 13 September 1993; accepted 13 March 1994

Abstract

The Middle to Upper Triassic Tanzhuang Formation represents part of the infill of the early Mesozoic Jiyuan-Yima Basin. The upper part of this stratigraphic unit records deposition within prevailing shallow lake conditions. Well-developed sequences crop out near Jiyuan, western Henan Province, central China. Six sedimentary facies clustered into two facies assemblages were recognized in the lacustrine section. Facies assemblage 1 consists of stacked coarsening-upward sequences composed, from base to top, of organic-rich shales (facies E, type I), laminated siltstones (facies A) and current-rippled laminated sandstones (facies B). Units of assemblage 1 record progradation of small mouth-bar deltas within a perennial open lacustrine system under temperate and humid conditions. Facies assemblage 2 lacks a clear vertical pattern and consists of interbedded fine-grained carbonates and siltstones (facies C); deformed and wave-reworked sandstones (facies D); organic-rich shales (facies E, type II) and clayey mudstones (facies F). The assemblage also represents a perennial, hydrologically-open, shallow lacustrine system, but characterized by strong seasonal climatic control. Water stratification probably occurred in several periods of the lake history. Pangaean megamonsoonal influence is envisaged to explain the strong seasonality imprint evidenced toward the upper part of the Tanzhuang lacustrine column.

Introduction

More than 140 Mesozoic to Cenozoic fault-controlled lacustrine basins are present in central and southeastern China, some of which contain abundant oil and gas reserves (Li & Luo, 1990). In most cases, these depressions were formed in response to strike-slip movements (Hsü, 1989; Zhu, 1989; Lin *et al.*, 1991). Basin-fills represent a wide variety of environments, such as alluvial fans, fan deltas, deltas, fluvial, and shallow and deep lakes. Li & Luo (1990) pointed out that from a structural and lithologic standpoint these lake basins are characterized by distribution along deep fault zones, widely distributed thick source rocks, well developed sand bodies, high geothermal gradients and multiple-trap styles.

The Jiyuan-Yima Basin is located in western Henan Province, central China (Fig. 1). It contains Triassic and Jurassic non-marine sediments, including relatively thick lacustrine deposits. The basin is currently divided into two sub-basins: Jiyuan and Yima, north and south of the Yellow River, respectively. The Tanzhuang Formation (Middle to Upper Triassic) records part of the infill of the Jiyuan sub-basin. The upper part of this formation represents deposition in a shallow perennial, hydrologically open lake (Mángano *et al.*, in review) and is well exposed southwest of Jiyuan city, north of Yellow River (Fig. 1).

The aim of this paper is: (1) to document the sedimentary facies of the upper part of the Tanzhuang

* This is the fourth paper in a series of papers published in this issue on 'Climatic and Tectonic Rhythms in Lake Deposits'.

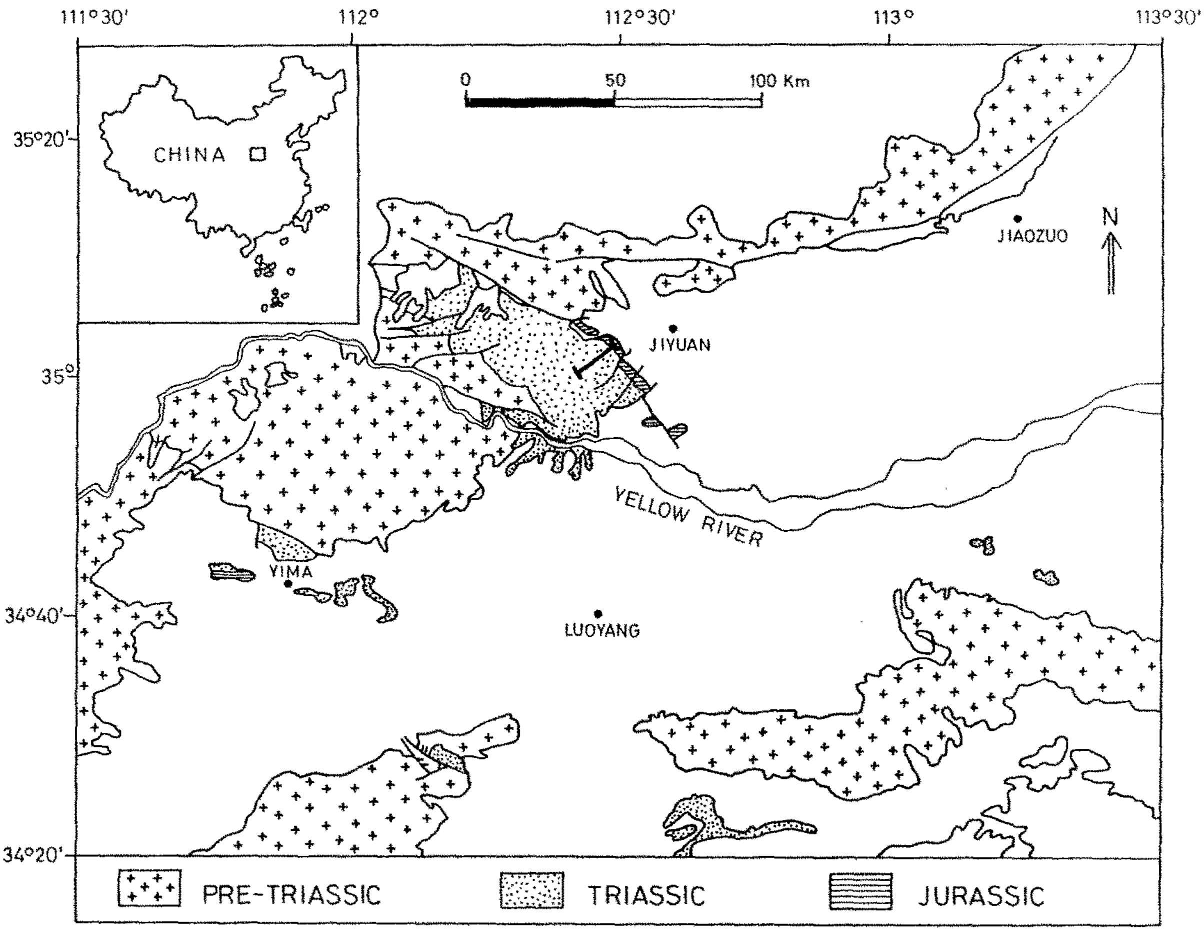

Fig. 1. Geological map of the Triassic lacustrine deposits of the Jiyuan-Yima Basin, showing the location of the section illustrated in Fig. 10.

Formation and (2) to discuss their depositional setting and the climatic controls on sedimentation.

Regional framework

The Jiyuan-Yima Basin is one of several nonmarine basins in central and southeast China. It hosts sediments of Middle Triassic to Middle Jurassic age and may be regarded as part of the Ordos Megabasin. The stratigraphy and paleontological content of the Jiyuan-Yima Basin was summarized by Zhou & Li (1980), Kang *et al.* (1984, 1985), and Hu (1991). Basement rocks consist of Permian clastic sediments deposited in deltaic environments. The two sub-basins (Jiyuan and Yima) were connected during the Triassic and later separated by the Yellow River fault in the Jurassic. Different lithostratigraphic units have been defined by Chinese workers for each sub-basin (Fig. 2). In particular, the Mesozoic column of the Jiyuan sub-basin is divided into two Triassic formations and three Jurassic formations, which encompass different nonmarine environments (Fig. 3).

The Jiyuan-Yima Basin was formed after the Early Indosinian Movements (Middle Triassic), which dramatically changed the tectonic configuration of southeastern China. These tectonic movements were produced by the accretion of the southern Yangtze Platform (South China Block) to the North China Block (Fig. 4) (Wang, 1985). Since the Triassic-Jurassic boundary (about 200 m.y.), the area has been affected by intense strike-slip motions and small continental fault-related basins have been emplaced in central and southeast China (Li & Luo, 1990). Evidence strongly suggests that the Jurassic sedimentation took place in a narrow pull-apart basin. However, the Triassic tectonic framework is still far from clear (Buatois *et al.*, in review; Mángano *et al.*, in review). Triassic deposits

JIYUAN-YIMA BASIN STRATIGRAPHY			
PERIOD	EPOCH	JIYUAN SUB-BASIN	YIMA SUB-BASIN
JURASSIC	MIDDLE	MAWA FORMATION	DONGMENGCHUN FORMATION
		YANGSHUZHUANG FORMATION	YIMA FORMATION
	LOWER	ANYAO FORMATION	BASAL CONGLOMERATE BEDS
TRIASSIC	UPPER	TANZHUANG FORMATION	SHIFU FORMATION
	MIDDLE	CHUENSHUYAO FORMATION	CHUENSHUYAO FORMATION

Fig. 2. Stratigraphy of the Mesozoic Jiyuan-Yima Basin. Based on Zhou and Li (1980); Kang *et al.* (1984, 1985); Wu (1985) and Hu (1991).

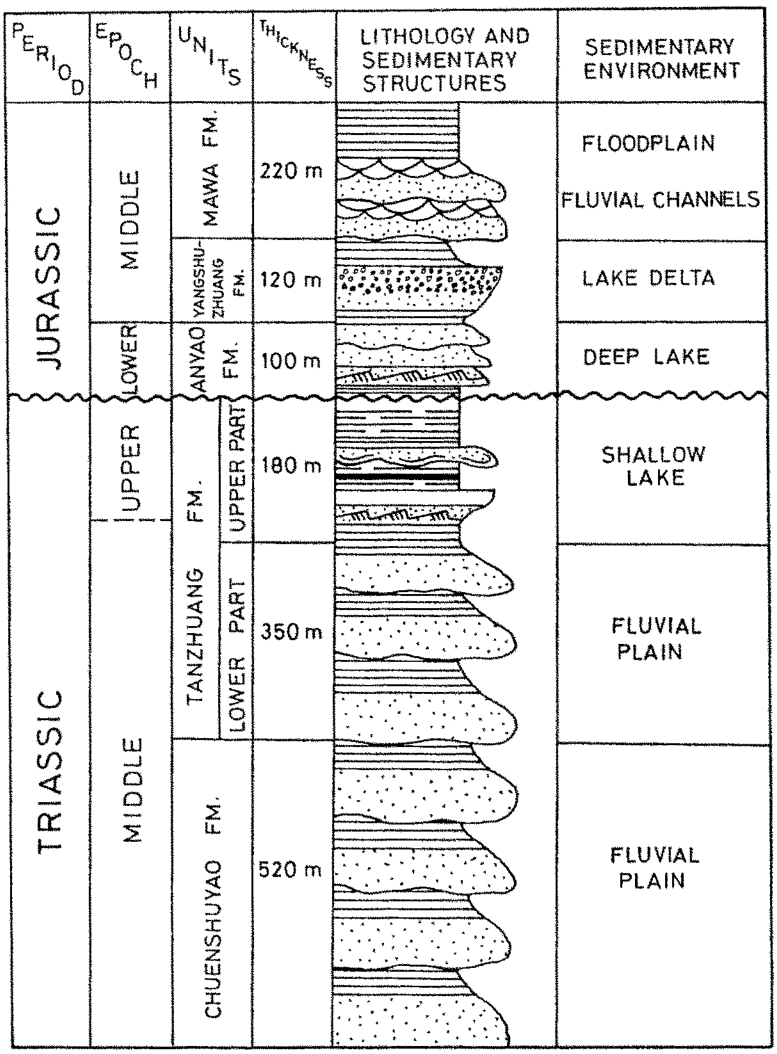

Fig. 3. Summary of the stratigraphy and sedimentary environments of the Mesozoic of the Jiyuan Sub-Basin (Based on Mángano *et al.*, in review and references therein).

of the northern Jiyuan sub-basin and the southern Yima sub-basin show significant changes in facies associations. Different stratigraphic units were considered for each sub-basin (Fig. 2). These facies variations probably indicate an asymmetric configuration of the whole Jiyuan-Yima Basin. Although the Triassic sedimentation may have been developed during an early stage of the pull-apart basin, the regional extension and relatively low subsidence rate may suggest more likely a post-collisional intracratonic downwarp basin, probably related with the formation of the Palaeo-Qinling mountain range (Fig. 5) (Wang, 1985).

During the Middle Triassic, the basin was infilled with alluvial and fluvial sediments, and the formation of standing waterbodies was relatively rare. These deposits comprise the Chuenshuyao Formation and the lower part of the Tanzhuang Formation (Hu, 1991; Sun, 1992). During the Middle to Late Triassic, sedimentation took place in a shallow and perennial lake, recorded by the upper part of the Tanzhuang Formation (Sun, 1992; Mángano *et al.*, in review).

Coincident with the Triassic-Jurassic boundary, strike-slip tectonism occurred in the area. The southern margin of the Jiyuan sub-basin was characterized by a high relief fault scarp, whereas the northern side probably had a less-pronounced topography. During the Early Jurassic, coarse-grained alluvial fan and fan delta systems were developed in the southern Yima area, close to the high relief scarp, whereas turbidity current deposition in a deep lake took place in the northern Jiyuan area (Wu, 1985; Buatois *et al.*, in review). Fan delta and alluvial fan deposits are represented by the Basal Conglomerate Beds south of Yellow River and lacustrine sediments are recorded by the Jurassic Anyao Formation at the Jiyuan area. Information of both types of environmental settings comes also from several boreholes. This Early Jurassic sedimentation is thought to reflect the onset of tectonic subsidence along the basin-bounding faults during a transtensile regime (Buatois *et al.*, in review).

Coincident with the Early-Middle Jurassic boundary, the Yanshan movement took place, uplifting the Taihang Mountains (part of the Northeast China Highland) (Fig. 5). As a consequence of this renewed tectonic activity, modified drainage of fluvial systems funneled high amounts of clastics into the basin, overcoming subsidence. Buatois *et al.* (in review) suggested that this later evolutionary stage was probably related to a transpressive regime. During the Middle Jurassic, a delta complex prograded into the lake and fluvial systems were later formed across the basin. In the Jiyuan sub-basin, deltaic deposits are recorded by the Yangshuzhuang Formation and the overlying fluvial sediments are represented by the Mawa Formation. The coeval Yima and Dongmengchun Formations record this evolutionary stage in the southern Yima sub-basin. A new phase of tectonic movements coincident with the Jurassic-Cretaceous boundary was probably responsible of the basin closure.

The Tanzhuang Formation consists of mudstones, organic-rich shales, thin-bedded carbonates, siltstones and sandstones that host the *Danaeopsis-Bernoulia* flora considered of Late Triassic age (Hu, 1991). However, palynological analysis at Jiyuan section suggests a Middle to early Late Triassic age for the upper part of the Tanzhuang Formation (G. Ottone, written communication, 1993). The upper 180 m of this formation was formed in a shallow permanent lake. The Tanzhuang Formation is underlain by the Chuenshuyao Formation and paraconformably overlain by the Lower Jurassic Anyao Formation (Hu, 1991). Palynological data suggest that the late Late Triassic may not be recorded within the succession. This time gap between the Tanzhuang and Anyao formations is probably related to the initial strike-slip tectonic activity roughly coincident with the Triassic-Jurassic boundary.

Sedimentary facies

Six sedimentary facies were recognized in the upper part of the Tanzhuang Formation: (A) Laminated siltstones; (B) Current-rippled laminated sandstones; (C) Interbedded fine-grained carbonates and siltstones; (D) Deformed and wave-reworked sandstones; (E) Organic-rich shales and (F) Clayey mudstones.

Facies A: Laminated siltstones and very fine-grained sandstones

Description: This facies is dominantly represented by laterally persistent, horizontally laminated greenish grey siltstones, forming units up to 5 m thick. Some lenticular thin coaly horizons, 2 to 4 cm thick, have been detected within the siltstones. Milimetric subhorizontal and oblique delicate root structures, and abundant plant debris are locally associated. Siltstone packages are characterized by fish scales, conchostracans, and well-preserved ostracodes (*Darwinula* cf. *D. shensiensis*, *Darwinula* cf. *D. contracta*, *Darwinula* spp., *Shensinella* sp., *Tungchunia*? sp., *Gompho-*

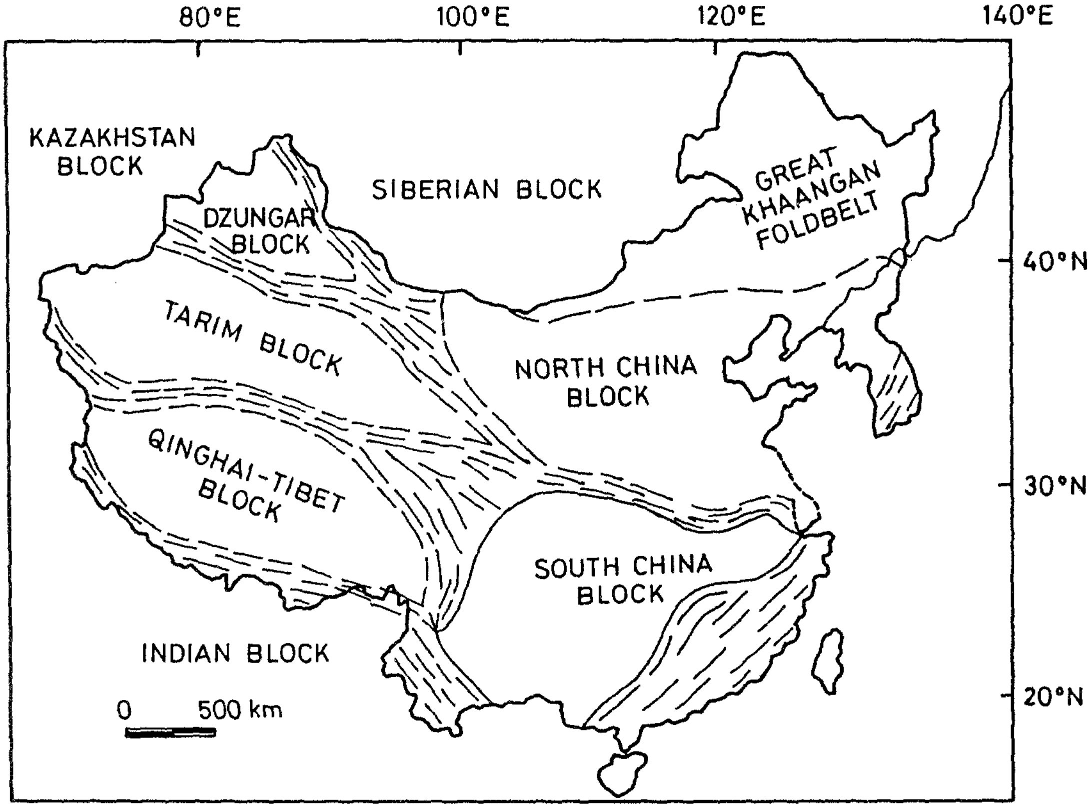

Fig. 4. Tectonic provinces of China (after Steiner *et al.*, 1989).

cythere? sp.), sparsely distributed within the siltstones (Wu Linyouling, pers. commun., 1992).

Interpretation: Absence of current and wave-induced structures, preservation of thin lamination and the fine grade of the material involved indicate deposition from suspension. The abundance of ostracodes and conchostracans indicates sedimentation in a shallow water low energy setting (Gore, 1988a). The local presence of rooted coaly horizons with abundant plant debris suggests that at least part of this facies may represent interdistributary bay sedimentation. The absence of features representing subaerial exposure also supports a subaqueous origin (Gore, 1988b, c).

Facies B: Current-rippled laminated sandstones
Description: This facies consists of conspicuous sandstone units, 0.6 to 8 m thick, lenticular at the scale of several tens of metres. The underlying laminated siltstones (facies A) pass up gradationally into a sandstone bed which commonly coarses upwards from very fine to medium or exceptionally coarse-grained sandstones (Fig. 6A, B). An ideal sequence of this facies shows current-rippled and climbing-rippled lamination in the finer lower part that passes up into planar lamination and culminates with planar cross-bedded or trough cross-bedding in the upper coarser material. The thickness of an individual bed ranges from 0.2 to 2 m, but beds are frequently stacked forming up to 8 m thick bedsets. Between sandstone beds, there are siltstone or silty sandstone partings. Soft-sediment deformation is locally present, particularly in the thickest units, forming load-based massive beds. Trace fossils (*Arenicolites*, thin grazing trails) and plant-rich horizons are commonly found at the top of the bedset. In a few cases, mudcracks occur at the silty top of sandstone units (Fig. 6C). Many sandstone bedsets show predominant development of the current-rippled interval, associated with climbing-rippled lamination (Fig. 6D) or current-rippled tops (Fig. 6E). More rarely, wave rippled-laminated sandstones occur at the top of the bedsets (Fig. 6F).

Interpretation: The general features previously described allow interpretation as lacustrine deltaic mouth-bar deposits. The vertical gradation from sus-

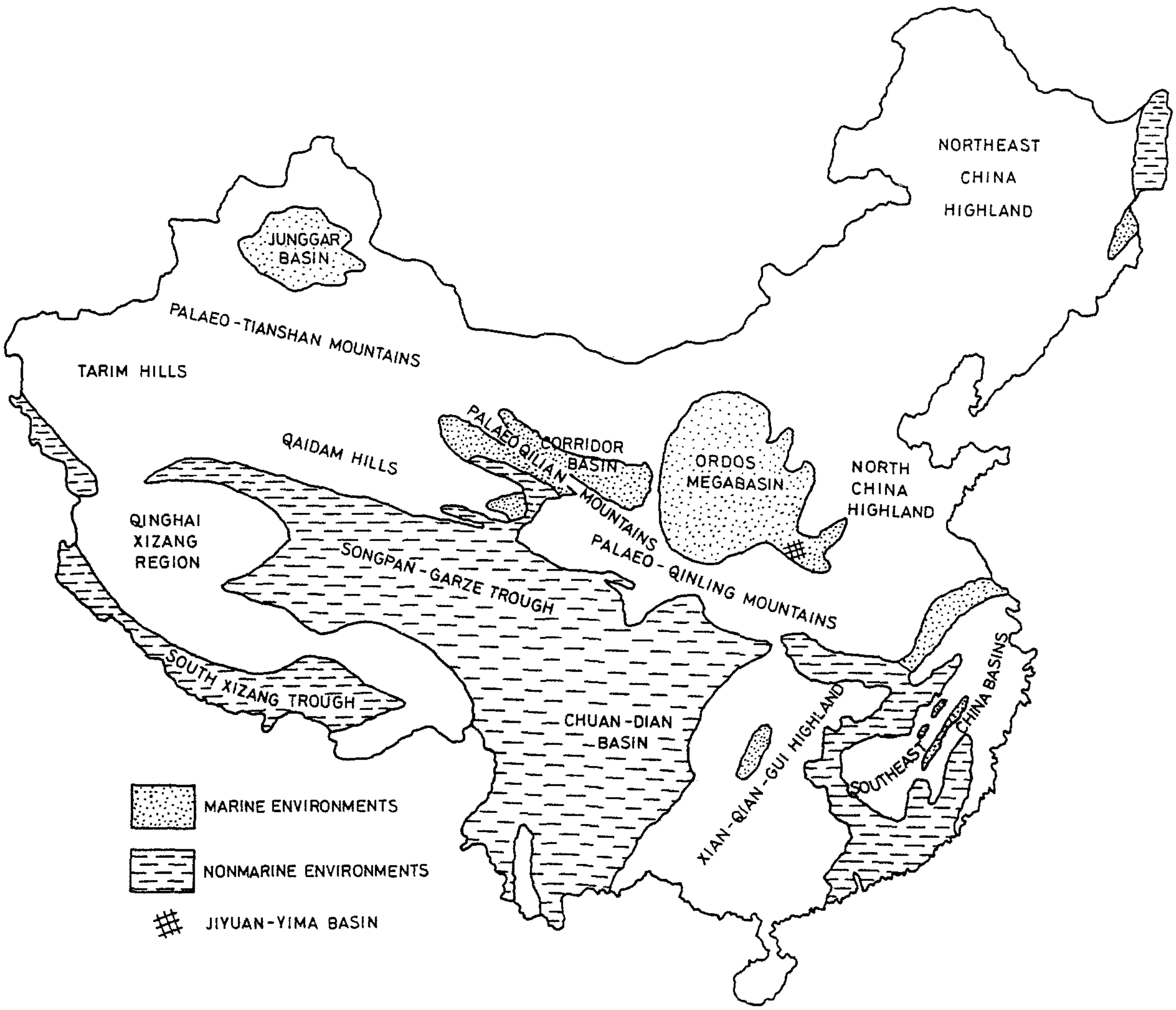

Fig. 5. Paleogeographic map of China during the Late Triassic (based on Wang, 1985).

pension deposits through current-rippled and climbing-rippled laminated sandstones to planar laminated, planar cross-bedded and occasionally trough cross-stratified sandstones represents a shallowing upward trend, which evidences the progradation of a mouth bar. Isolated thin bedsets dominated by current-rippled laminated sandstones may represent mouth-bar toes. The presence of wave rippled-laminated sandstones capping some mouth-bars probably records the action of waves shoaling over the top of the prograding sandstone body. In lacustrine settings, similar facies were described by Farquharson (1982) from the Cretaceous of Antarctic Peninsula.

Facies C: Interbedded fine-grained carbonates and siltstones

Description: This facies consists of an alternation of yellowish white carbonate laminae (0.05–0.4 cm thick) and greyish green laminated siltstones (0.5–1.5 cm thick), forming intervals up to 2.6 m thick (Fig. 7A). Beds are sharp-based and laterally persistent. Bioturbation is virtually absent with the exception of post-depositional, unlined, constricted, vertical burrows of *Skolithos serratus* (= *Stipsellus*).

Interpretation: In lacustrine settings, carbonate is mainly supplied from bio-induced precipitation by phytoplankton, and from resedimentation, although inorganic precipitation may also occur during lake turnover (Kelts, 1988; Platt & Wright, 1991). No

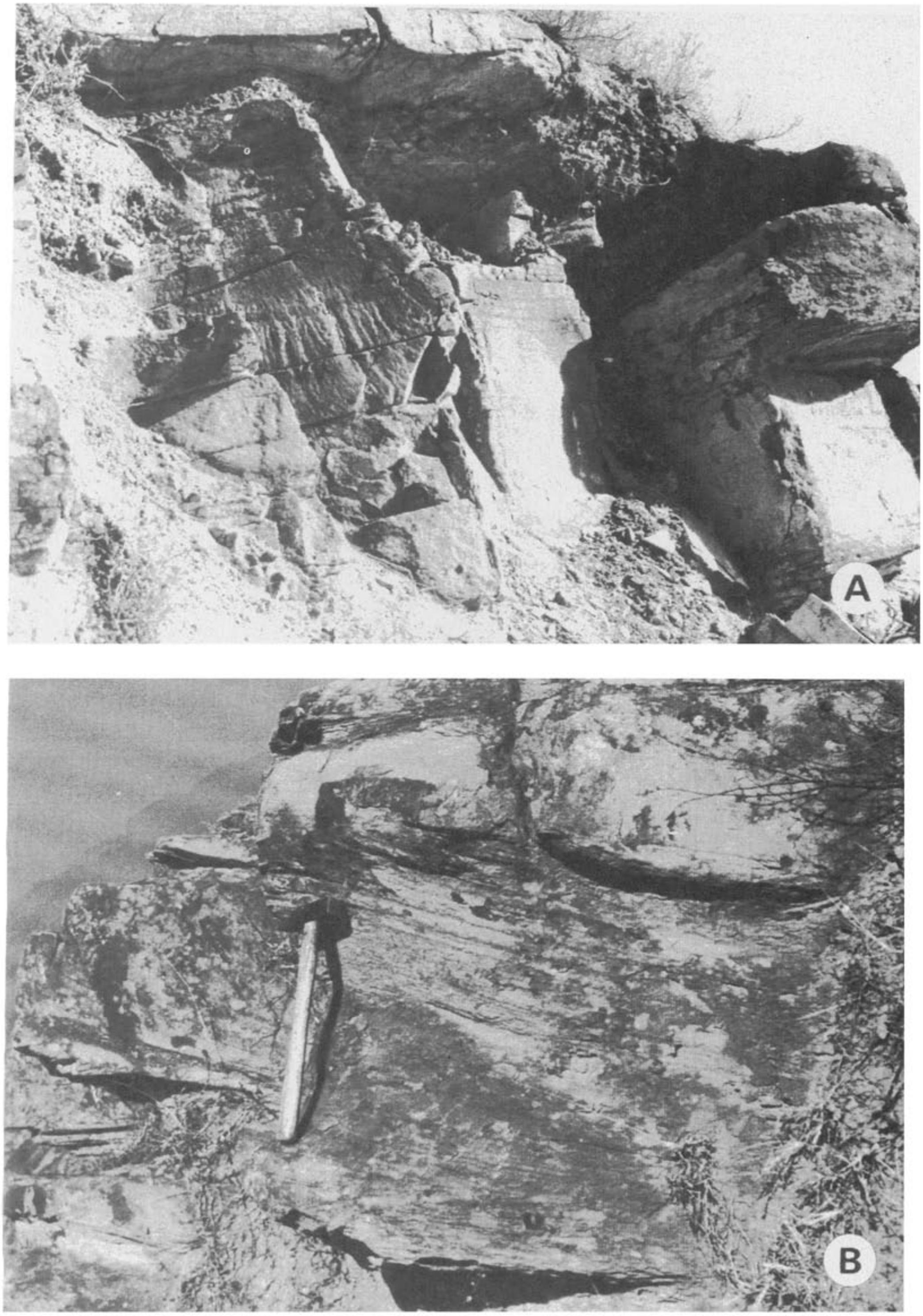

Fig. 6. Facies Assemblage 1. A, current–rippled laminated sandstone facies (B), forming a coarsening upward sequence. B, detailed view of facies B, showing planar cross-bedded sandstones that pass upwards into trough cross-bedded sandstones. C, desication cracks at the top of a facies B sandstone body. D, detailed view of a current rippled and climbing ripple-laminated interval of facies B. E, current rippled top from a facies B sandstone body. F, detailed view of wave ripple lamination in a facies B sandstone unit.

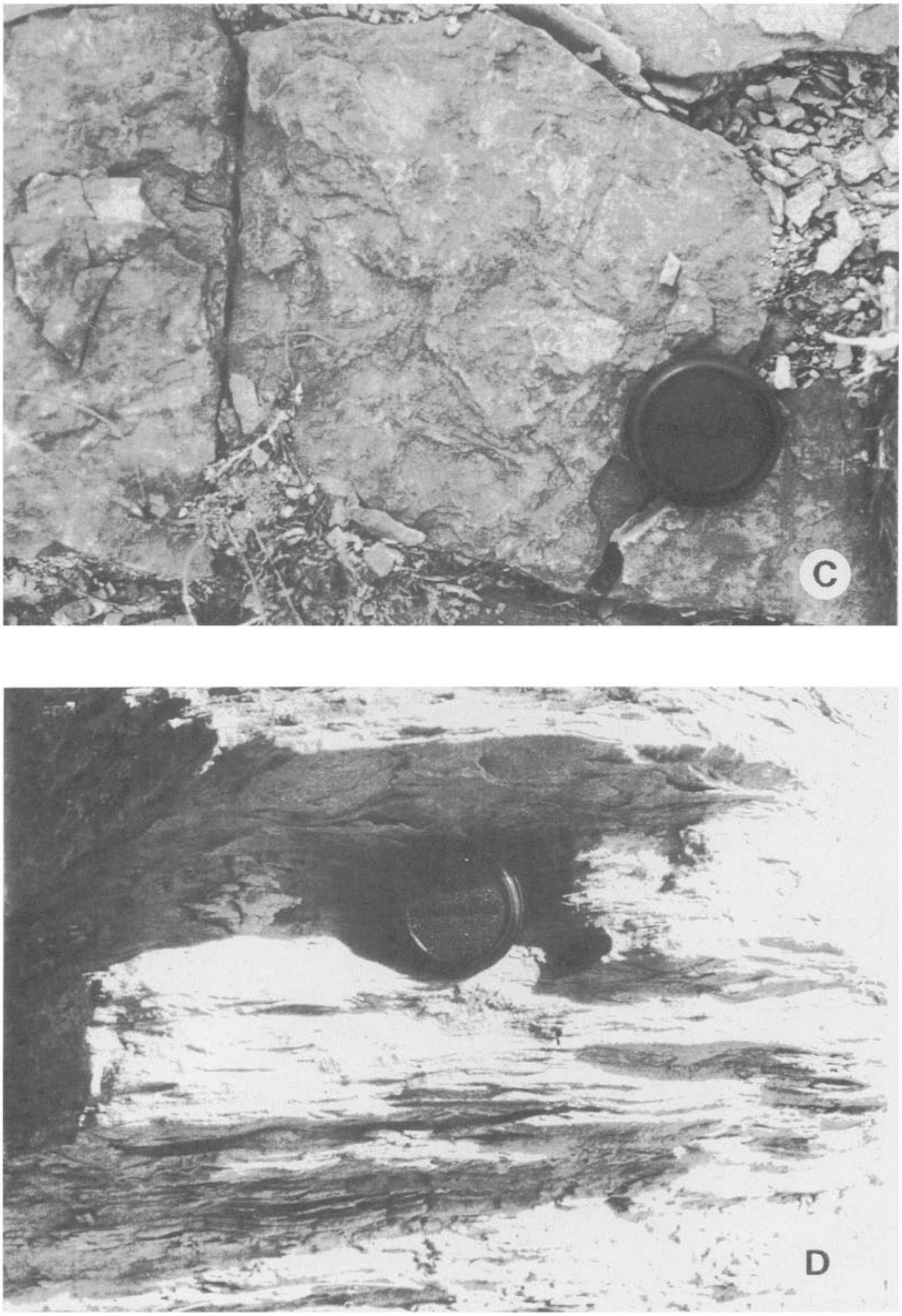

Fig. 6. Continued.

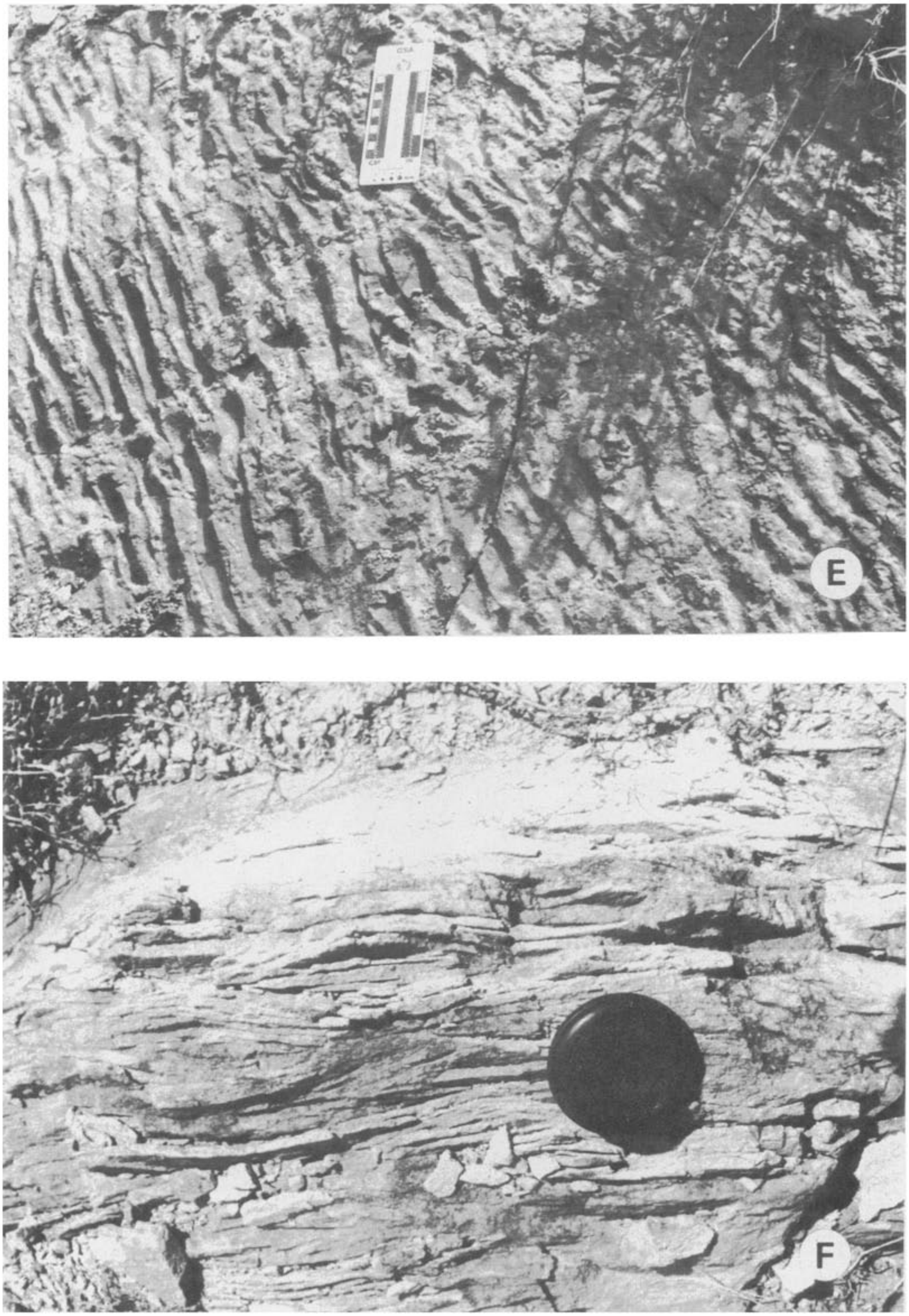

Fig. 6. Continued.

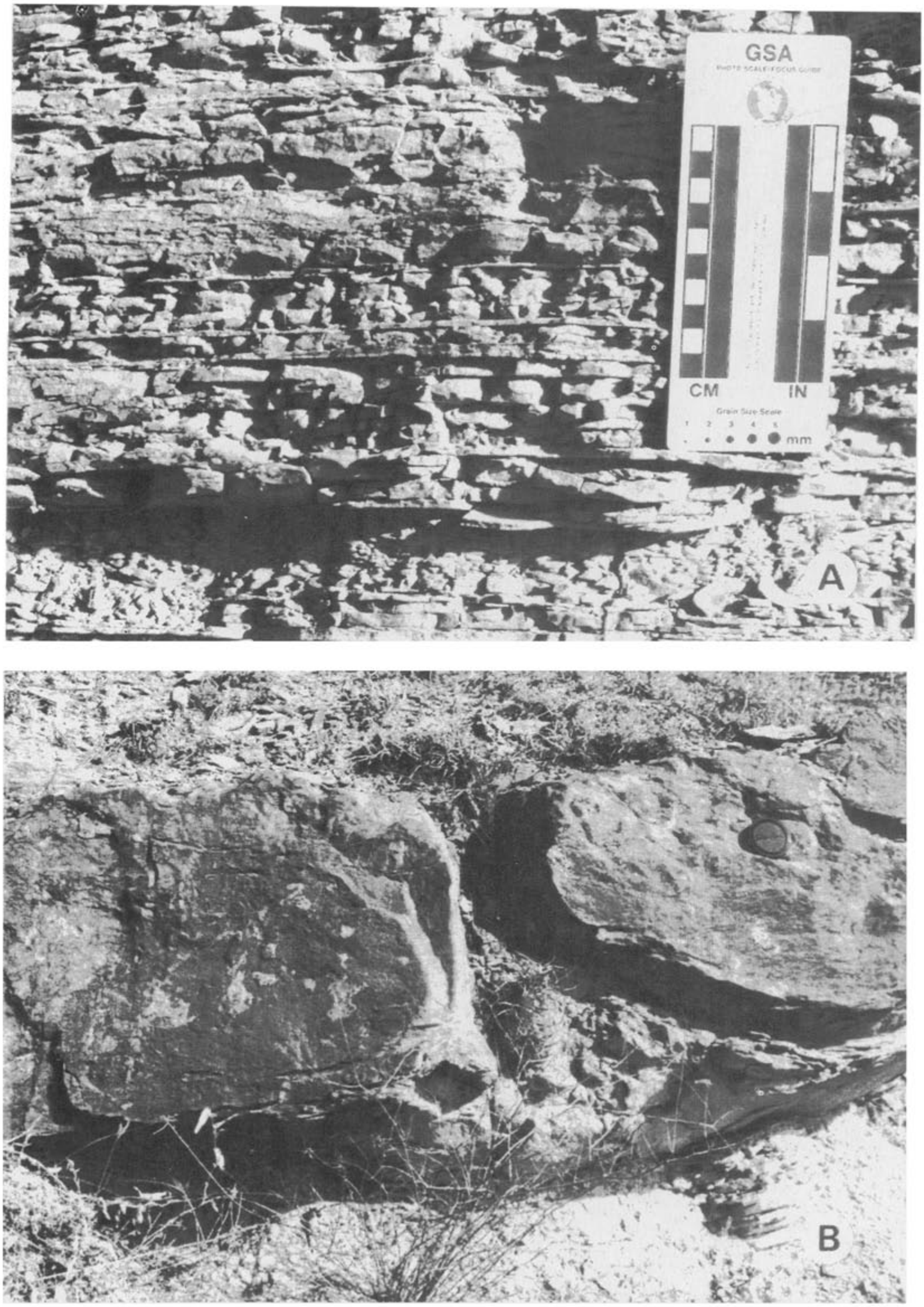

Fig. 7. Facies Assemblage 2. A, Interbedded fine-grained carbonate and siltstone facies (C) B, deformed and wave-reworked sandstone facies (D). Detailed view of load bases and pseudonodules. C, Interbedded facies C and D, which are overlain by a relatively thick package of organic-rich shale facies (E). D, Bedding plane view of the top of a facies D sandstone bed, showing straight wave ripples of chevron type.

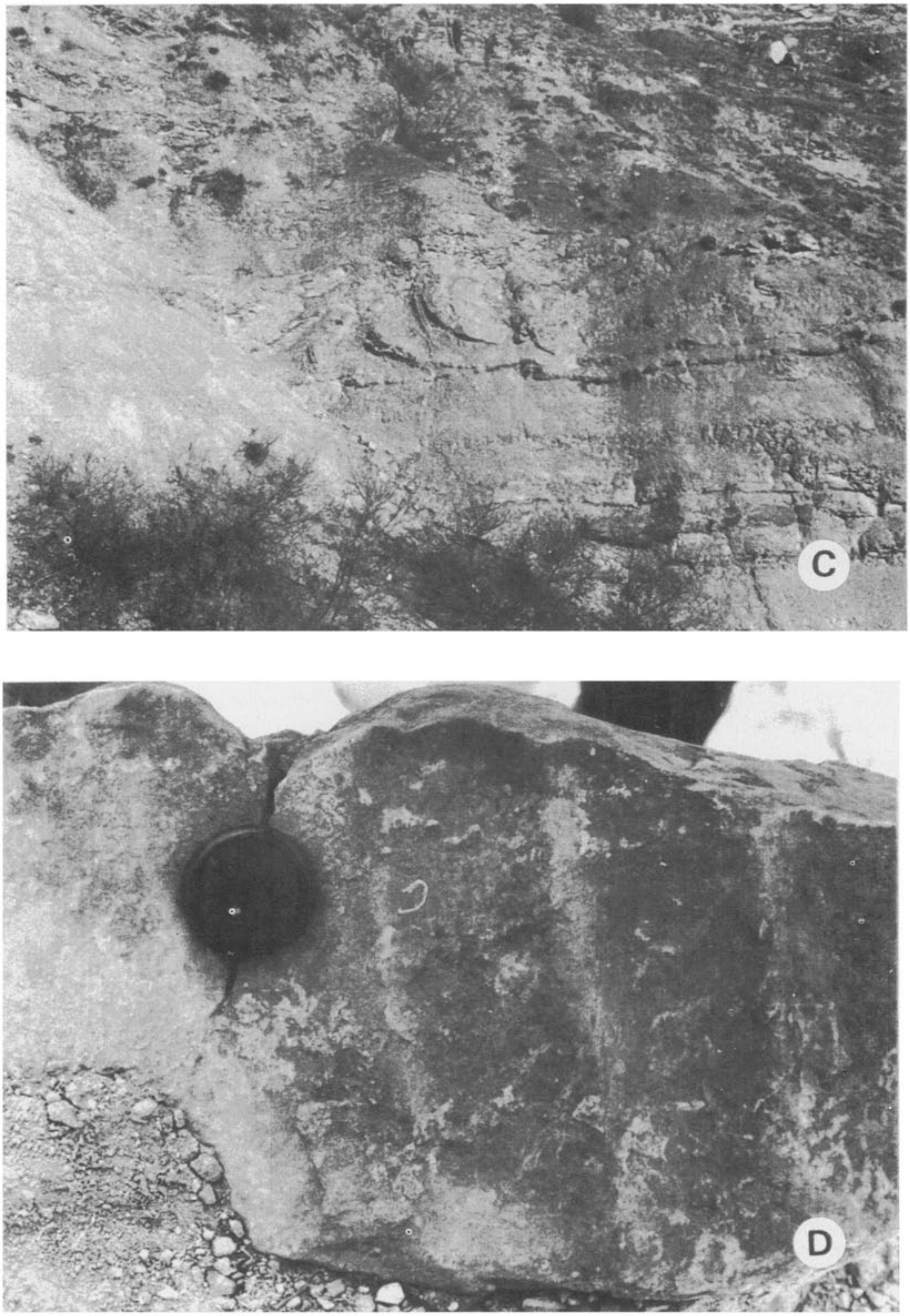

Fig. 7. Continued.

matter which genesis was involved, the presence of these carbonates interbedded with clastic deposits represents drastic seasonal changes in carbonate concentration and detrital influx, that led to periodic carbonate precipitation. Laterally persistent laminite fabrics can only be preserved in situations of slow, fine-grained, suspension-dominated deposition with inhibited burrower activity. This situation is commonly found below storm wave base under oxygen-depleted conditions that prevent from profuse bioturbation. However, the presence of associated wave-rippled event beds (facies D) punctuating the laminated sediments points out that, at least, part of the packages were deposited in nearshore water. The local presence of vertical burrows cross-cutting the laminated deposits probably reflects an improvement in the oxygen content and relatively firm substrates.

Facies D: Deformed and wave-reworked sandstones

Description: Facies D occurs as laterally persistent syndepositionally deformed fine-grained sandstone units, up to 1.8 m thick (Fig. 7B). Individual beds vary from a few centimetres to 0.7 m and commonly fine upwards. Thicker units are the product of amalgamation. Most sandstone beds show load casts. Very thin silty sandstone partings are frequently observed. An ideal facies D sandstone bed consists of three divisions (Fig. 8): a parallel laminated basal division (P) that passes upward abruptly into a deformed interval (D) and culminates with a wave-rippled lamination division capped by well-preserved oscillatory ripples (Fig. 7D), commonly of chevron type (R). Wave ripple length averages 8.6 cm and amplitude is about 4.6 cm. The ripples at the top are typically straight (Fig. 7D) to slightly sinuous and quasi-symmetrical. However, in some beds interval R is formed by current-rippled lamination with sinuous asymmetrical ripple trains at the top. The complete facies D bed sequence is less common than incomplete variants. In many cases, the lower and the upper divisions are missing and the depositional unit is represented by a load-based deformed sandstone bed. Indeed, thin sharp-based beds of normally graded, very fine-grained sandstones are locally common. Exceptionally, intraclasts have been detected at the lower part of relatively thick sandstone bodies. Postdepositional burrows (*Skolithos*, *Palaeophycus*) were detected at the top of some beds.

Interpretation: Sharp basal contacts and sequence of structures of these sandstone beds indicate event sedimentation, probably related to episodic rainfalls. This type of event beds has been called inundites and are formed when river floods enter into waterbodies (Seilacher, 1991). In the analyzed case, these deposits record the entering of ephemeral sheet-floods into a shallow lake. The presence of syndepositional deformational structures suggests high rates of sedimentation. The existence of symmetrical ripple tops indicates that the sands were reworked by waves in a nearshore lacustrine setting. However, the presence of sandstones entirely formed by current ripples may indicate, at least for some of the beds, sedimentation below wave base. Symmetrical ripples at the top of sandstone beds and the absence of mudcracked surfaces and related pedogenic horizons indicate subaqueous deposition (Gore, 1988b, c). Thin normally graded sandstone interbeds within facies C probably represent distal expressions of the inundites. The occurrence of postdepositional burrows reflects colonisation of opportunistic suspension feeders. A similar facies was described by Gore (1988b, c) from the early Mesozoic Culpeper Basin in Virginia.

Facies E: Organic-rich shales

Description: This facies consists of dark grey to black, thinly laminated organic-rich shales, forming packages 2 to 50 cm thick (Fig. 5C). No varve-like couplets have been detected (Hentz, 1985; Gore, 1988a, b). According to palynologic content and package thickness, two distinct types of organic-rich shales (ORS) can be distinguished. *Type I-ORS* is formed by thin packages of shales (2–20 cm thick) that host a palynomorph assemblage dominated by pteridosperm and coniferophyte bisaccate pollen grains (75–85%). Spores of pteridophytes, sphenophytes and lycophytes, together with monosulcate pollen grains and *Botryococcus* sp. are minor constituents. Wood remains and cuticles are common (E. G. Ottone, written commun., 1993). The organic matter is dominated by dispersed and finely detritic components ascribed to strongly degradated herbaceous plants. Plant input was high. Thermal maturity estimated from vitrinite reflectance is 0.93 TOC is 1.08 (H. Villar, written commun., 1993). *Type II-ORS* consists of conspicuous packages of shales (15–50 cm thick) characterized by a monotonous palynomorph assemblage composed of the green algae *Botryococcus* sp. (>90%). Minor constituents are another green algae (*Tasmanites* sp.), spores, cuticles and wood remains (E. G. Ottone, written communication, 1993). Fish scales are local-

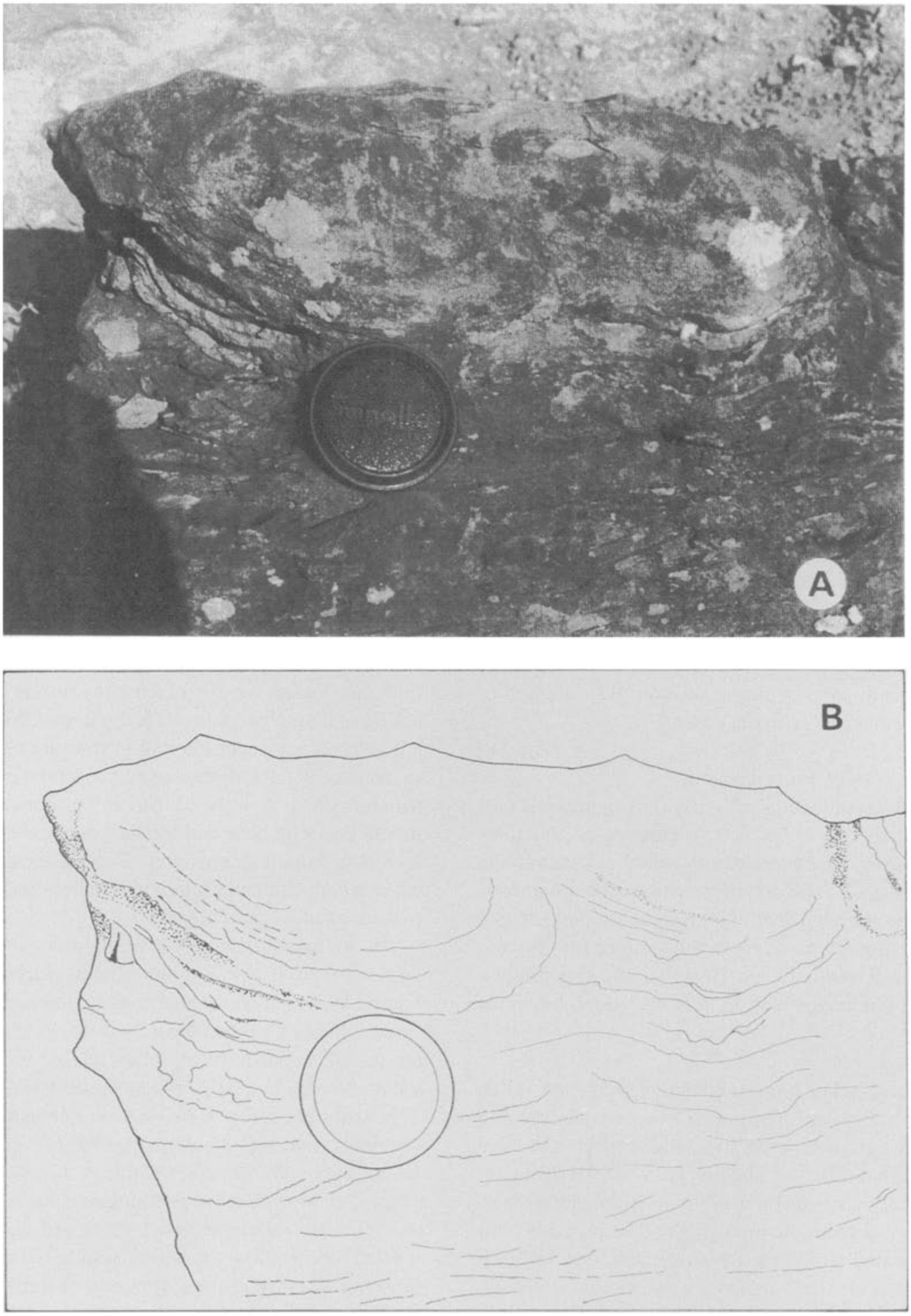

Fig. 8. Field photograph (A) and explanatory sketch (B) of a facies D event bed. Note the threefold division of the bed: a parallel laminated basal division (P) that passes upward into a deformed interval (D) and culminates with a wave-rippled top (R).

ly present. The organic matter is predominantly of amorphous-sapropelic type and was probably origined from algal precursors. Plant input was low. Thermal maturity estimated from vitrinite reflectance is 0.84 TOC is 1.87 (H. Villar, written commun., 1993).

Interpretation: Sedimentologic features of organic-rich shale facies indicate fallout deposition in a relatively quiet basin setting. The absence of megafauna and bioturbation suggests anoxic or near anoxic bottom conditions (Allen & Collinson, 1986; Gore, 1988b, c; Kelts, 1988). Reflectance data show that both types of organic-rich shales are well within the oil generation window. Contrast between type I and type II-ORS reflects differences in the predominant source of the organic matter. Type I-ORS is dominated by allochthonous material (pollen, spores, wood remains), indicating a significant extrabasinal supply. Association of type I-ORS with perennial river-derived deposits (facies A and B) suggests high and continuous clastic input into the lake. On the contrary, type II-ORS reflects low dilution of autochthonous organic supply, suggesting significant seasonal algae production (*Botryococcus* sp.) and low intrabasinal supply. This fact may give evidence of important changes in lake dynamics and climatic control.

Facies F: Clayey mudstones

Description: Facies F is present in the uppermost part of the Tanzhuang Formation. It consists of structureless light grey clayey mudstones, which occurs as units 0.6 to 2 m thick. The clayey mudstones are characterized by the abundance of plant fragments. No paleosol horizons, mudcracks or identificable trace fossils were detected within this facies. However, the structureless nature of this facies may indicate thorough bioturbation.

Interpretation: The environmental significance of this facies is still unclear. The poorly exposed outcrops and the absence of sedimentary structures make a reliable interpretation difficult. The fine grain size of the material indicates suspension deposition within a low energy setting, whereas the light grey colour suggests sedimentation under oxygen-depleted conditions. Facies F was more likely deposited in a very shallow water setting, probably within a mudflat.

Facies assemblages

Two distinct facies assemblages have been recognized in the upper part of the Tanzhuang Formation (Fig. 9). Assemblage 1 consists of facies A (Laminated siltstones), B (Current-rippled laminated sandstones) and locally facies E (Type I Organic-rich shales). Assemblage 2 is formed by Facies C (Interbedded fine-grained carbonates and siltstones), D (Deformed and wave-reworked sandstones); E (Type II Organic-rich shales) and F (Clayey mudstones).

Facies assemblage 1 is characterized by coarsening-upward sequences which are composed of (from bottom to top) type I organic-rich shales (facies E), laminated siltstones with thin coaly horizons (facies A) and fine to medium, exceptionally coarse-grained sandstones (facies B). Individual coarsening-upward sequences range from 2 to 8 m thick, but are commonly stacked, forming two distinctive stratigraphic intervals (0–35 m and 71–95 m; Fig. 10; see Fig. 11 for log key) within the lacustrine succession. Each sequence records the vertical gradation from suspension deposits to current and, more rarely, wave-reworked sediments, resulting from the progradation of deltaic mouth bars in a lacustrine setting. The variability of mouth bar deposits is illustrated in Fig. 12. In a few cases, an upper interval of trough cross-bedded sandstones occurs, representing the influence of a distributary channel in the central and proximal part of a mouth bar. The base and top of a sequence are sharp and record flooding episodes. This facies assemblage records deposition in a relatively shallow and perennial hydrologically open lake.

Facies assemblage 2 is typified by thick packages of type II organic-rich shales (facies E), and interbedded fine-grained carbonates and cohesive siltstones (facies C) punctuated by event sandstone beds (facies D). Towards the top of the succession, an interval dominated by clayey mudstones (facies F) occurs. This assemblage forms two well-defined stratigraphic segments (intervals 35–71 m and 95–175 m; Fig. 10). In contrast with facies assemblage 1, assemblage 2 lacks a clear vertical facies pattern. The bulk of the assemblage is thought to represent sedimentation in a relatively shallow lacustrine setting. The common presence of wave ripples at the top of sandstone beds indicates that at least part of the event sediments were deposited above wave base level in a nearshore setting (Fig. 13). Water stratification probably occurred at several times of the lake history, particularly during deposition of the lower stratigraphic interval of

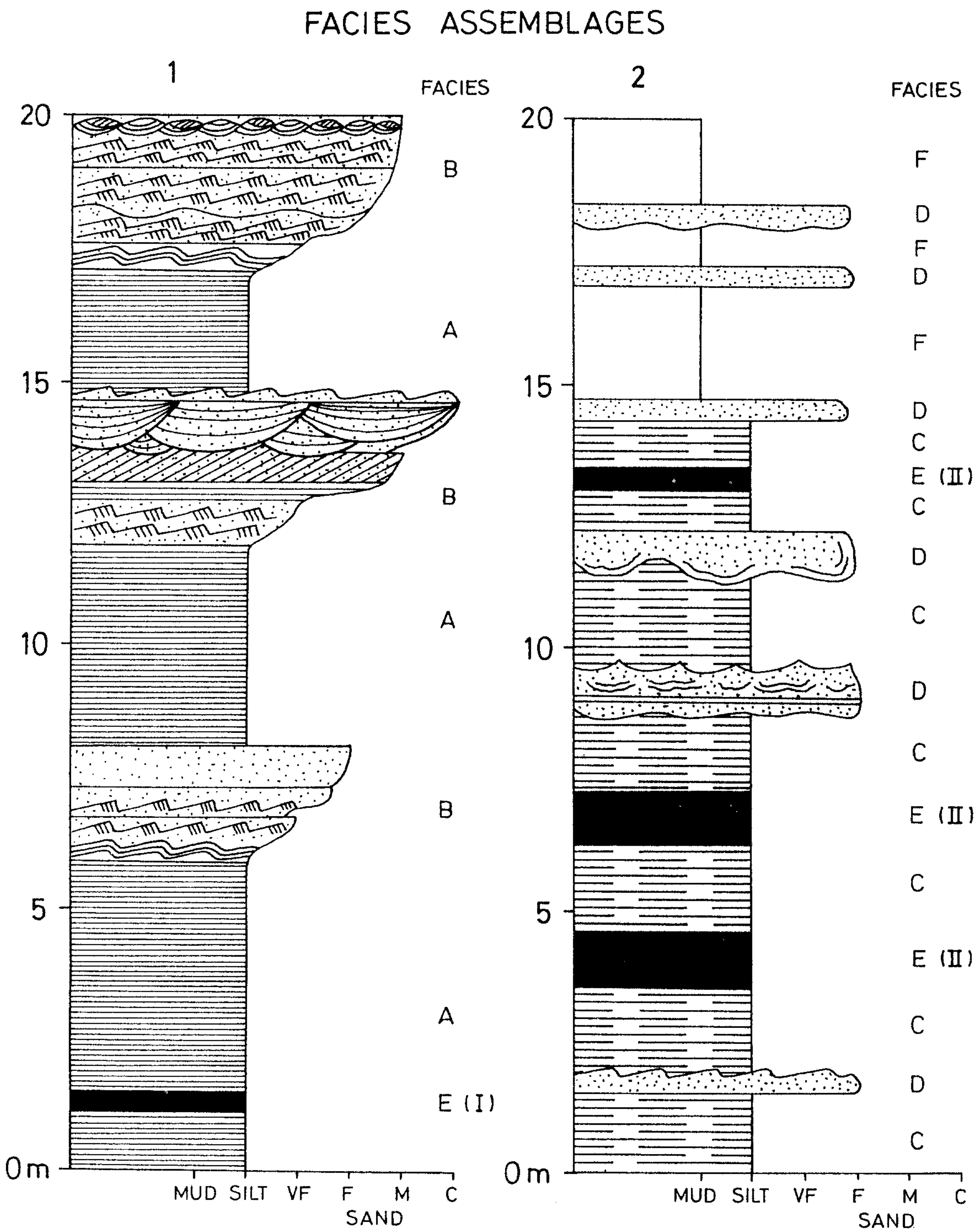

Fig. 9. Idealized sequences of Triassic lacustrine facies assemblages.

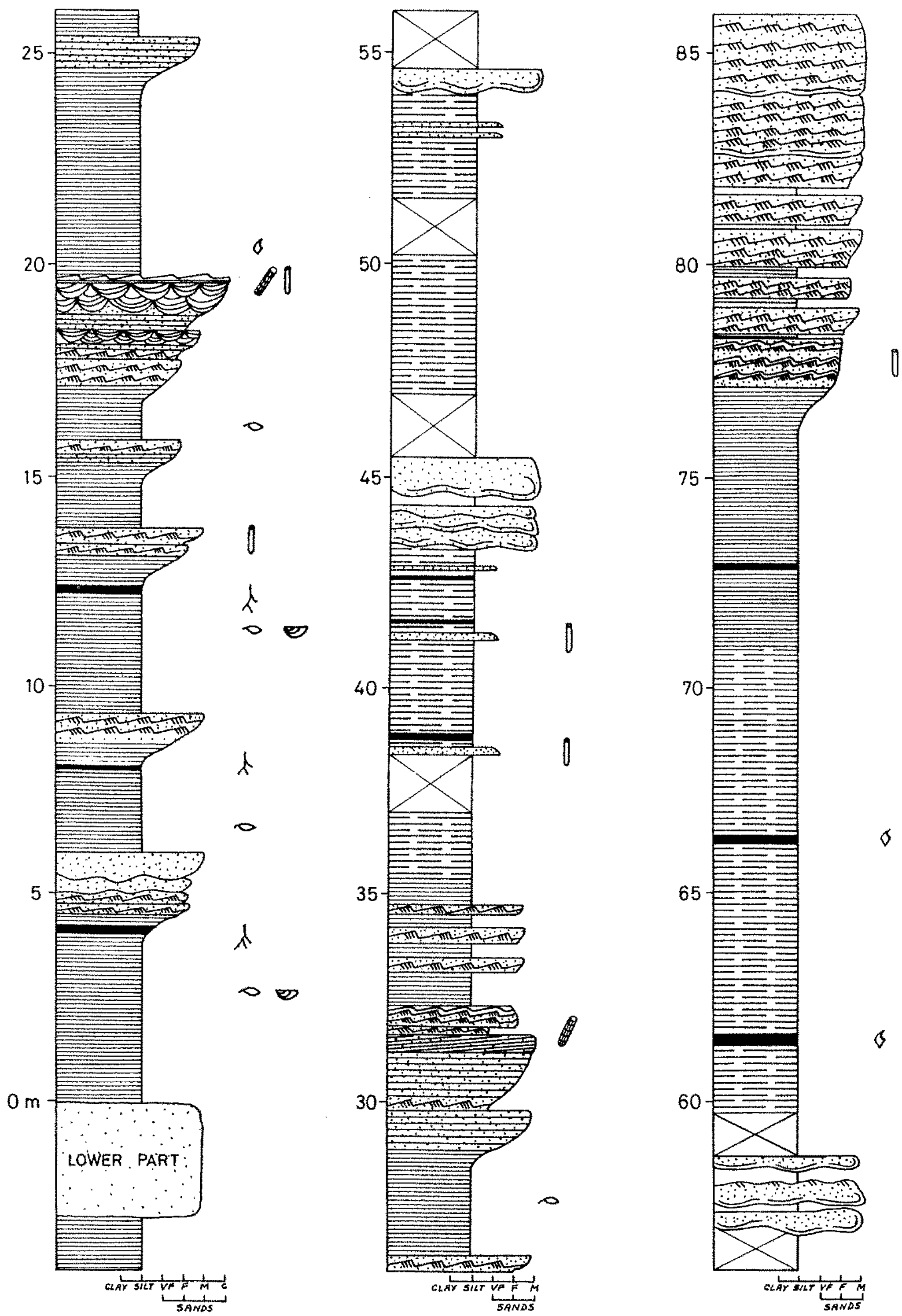

Fig. 10 a. Sedimentary logs of the upper part of the Thanzhuang Formation. Jiyuan section.

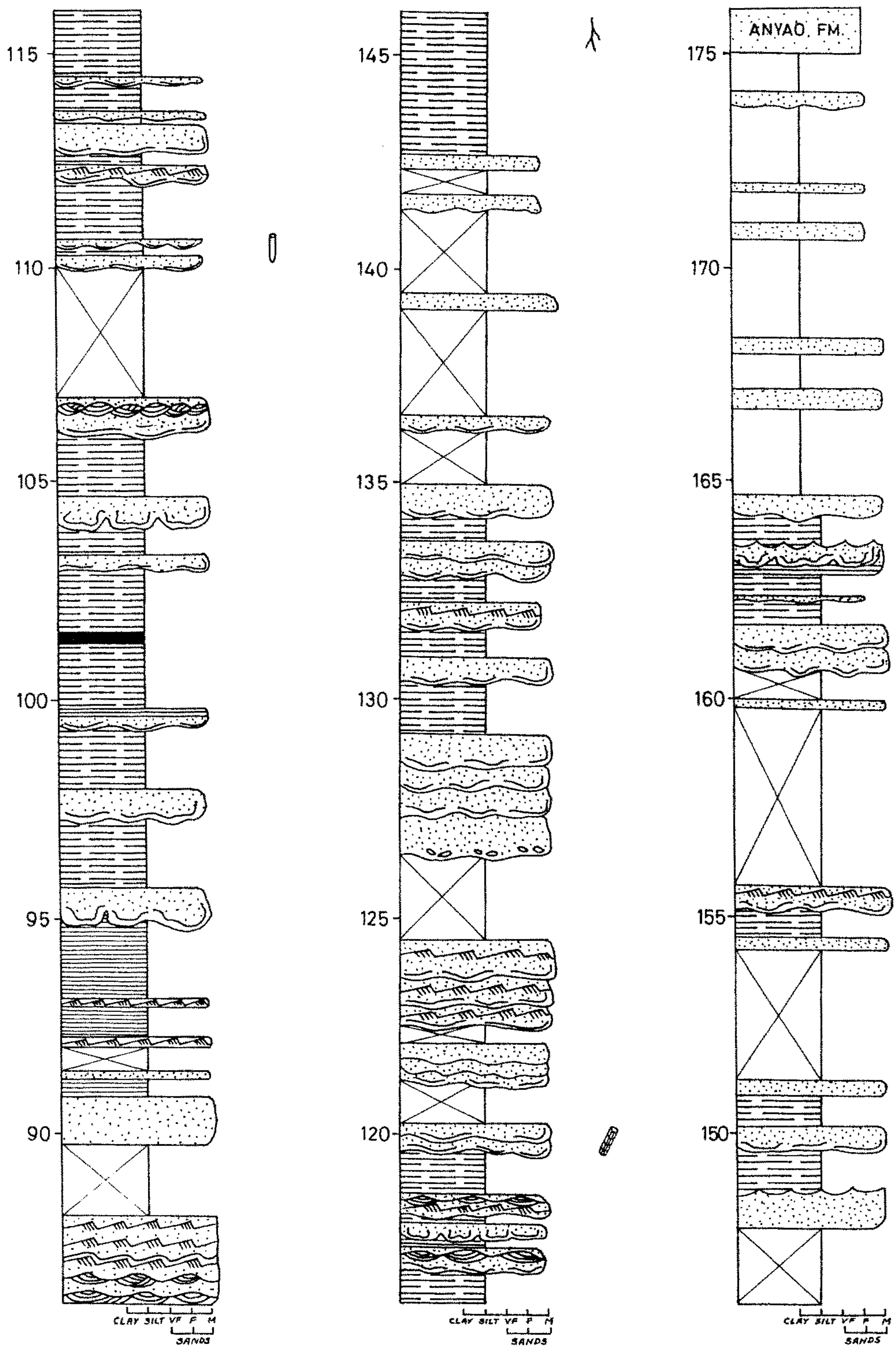

ANYAO. FM.
115
110
105
100
95
90
145
140
135
130
125
120
175
170
165
160
155
150
CLAY SILT VF F M
SANDS

Fig. 10 b.

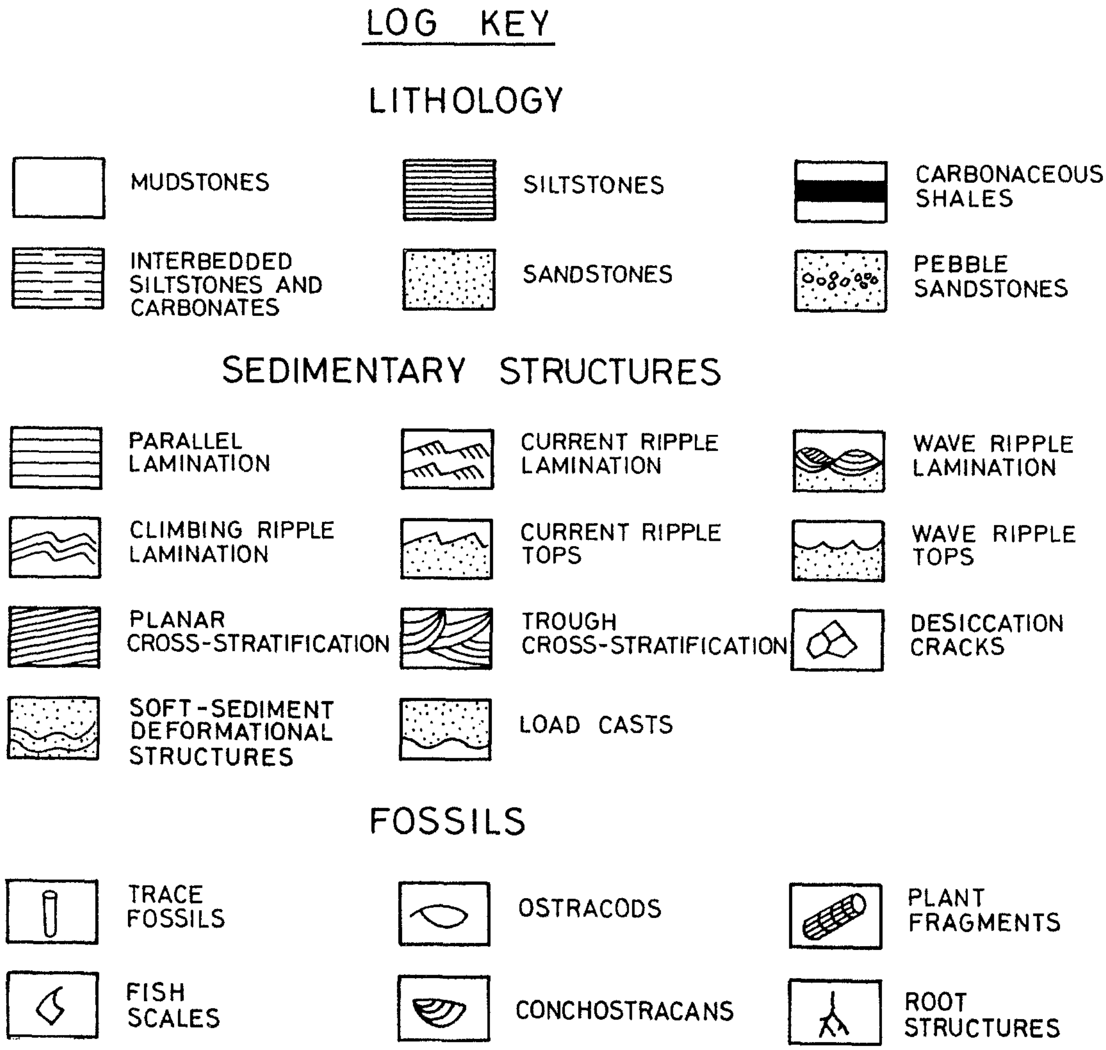

Fig. 11. Log references of Figs 3, 9, 10, 12 and 13.

facies assemblage 2 (Fig. 10; 35–71 m). Facies assemblage 2 also represents a perennial shallow lacustrine system, but characterized by strong seasonal rains. To establish the hydrologic regime during this phase of lake evolution requires further research. However, the absence of evaporites, cyclic transgressive-regressive sequences capped by subaerial exposure surfaces and relatively stable shorelines call for an open-basin lake (Gore, 1989).

Discussion

Tectonic processes permitted the Tanzhuang lake to develop, but climatic regime was the main control in its style and evolutionary history.

Environmental setting and lake dynamics

Units of assemblage 1 record progradation of small mouth-bar deltas within an open lacustrine system under temperate and humid conditions. The hydrodynamic mechanisms involved in deltaic sediment distri-

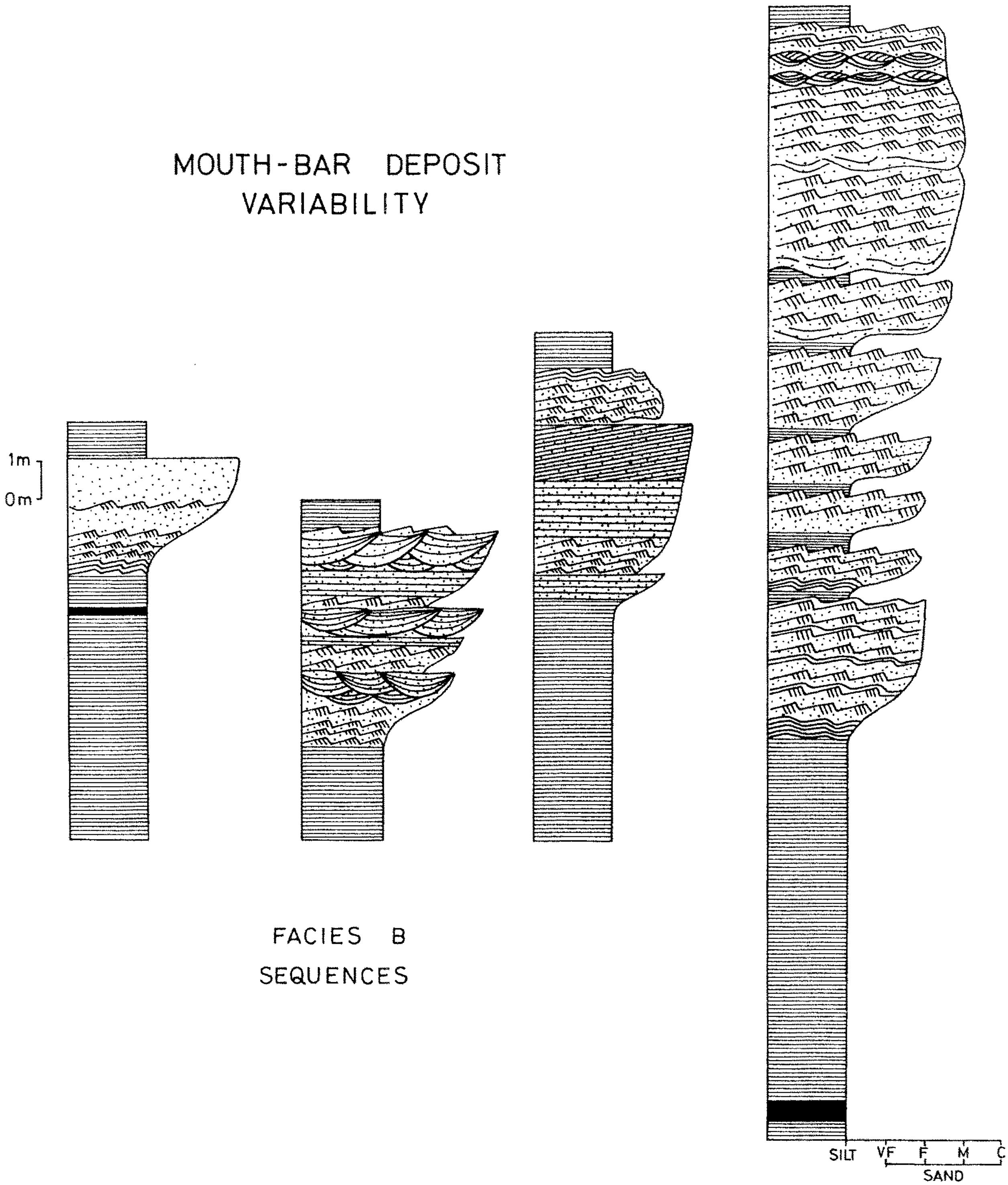

Fig. 12. Mouth bar deposit variability (facies B). Selected intervals from the Jiyuan section.

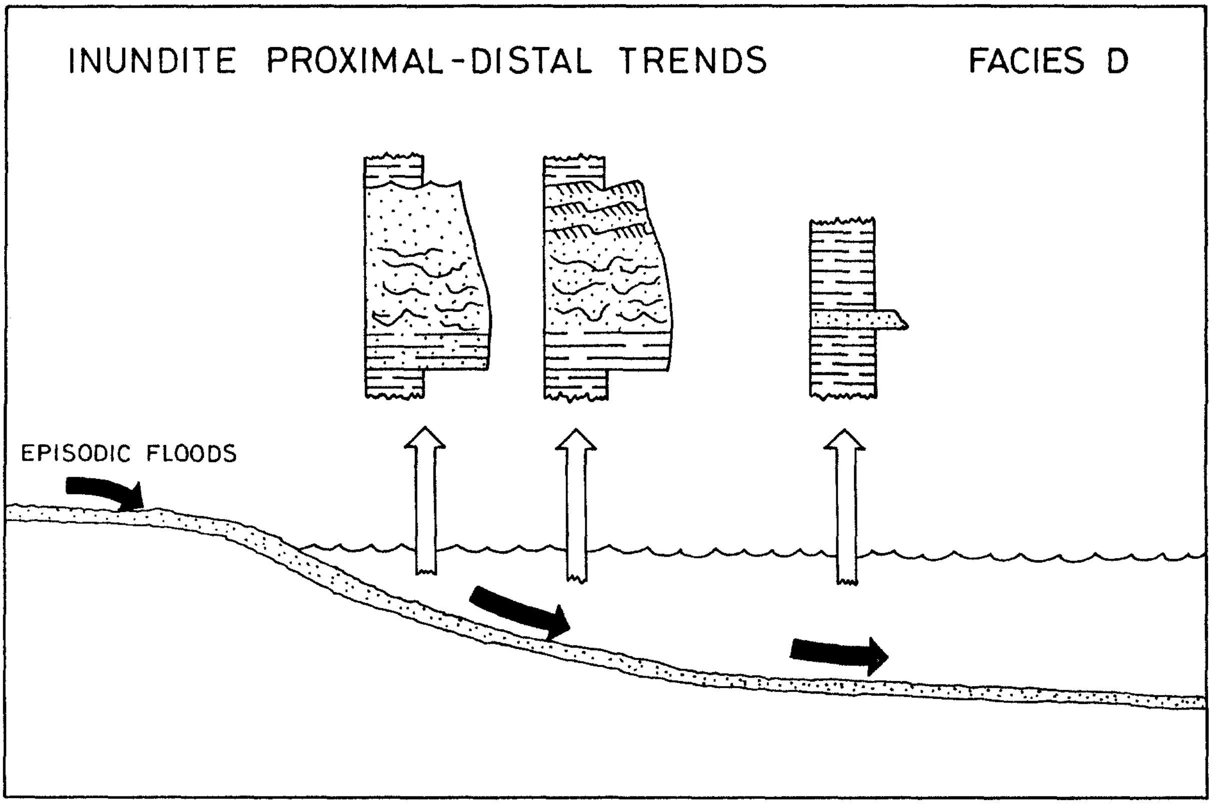

Fig. 13. Proximal-distal variability within event beds (facies D) of facies assemblage 2. Sandstone beds were generated from unidirectional episodic floods. Sands deposited in a nearshore setting were moulded by waves into wave-rippled lamination. Sandstone beds emplaced below wave base level are characterized by current-ripple structures. Farther into the lake, thin-bedded, normally-graded sandstone beds were formed.

bution have received much attention in the literature (e.g. Bates, 1953; Gilbert, 1975; Wright, 1977; Coleman & Prior, 1980). The river mouth is a dynamic sediment dissemination point, in which the effluent interacts with the waters of the receiving basin. The pattern of sediment distribution and processes involved depend on three major factors: (1) buoyancy of the river water resulting from density contrast between the effluent water and the basin water; (2) inertia of the river effluent water; and (3) friction between the effluent and the basin bed (Wright, 1977; Coleman & Prior, 1980). According to which of these three factors is the dominant, different patterns of distribution of river mouth sands are involved. Density contrast between the effluent and the basin waters is mainly significant in oceanic basins, where the high density saltwater contrasts with the river freshwater density.

When inertial forces are dominant in relatively deep lake basins, the effluent spreads as a turbulent jet. Deposits are typically quite thick and display well-defined bottomset, foreset and topset, resulting in the development of Gilbert-type deltas (Allen & Collinson, 1986). This river mouth mechanism has been mentioned in many lacustrine settings, such as the Permo-Carboniferous of India (Sen & Banerji, 1991); the Cretaceous of Antarctic Peninsula (Farquarson, 1982); the Eocene Green River Formation of Wyoming (Stanley & Surdam, 1978) and the Pleistocene of Canada (Shaw, 1975).

Finally, when sediment-ladden waters enter into a relatively shallow basin, bottom friction plays the major role and turbulent diffusion is restricted to the horizontal. According to Bates (1953) terminology, we can characterize a sediment-ladden effluent entering into the less dense lacustrine waterbody as a hyperpycnial flow. This process results in a mouth bar delta system with a bifurcated channel pattern. Processes involved and sediment distribution pattern of the mouth bars herein described give evidence of a friction-dominated river mouth depositional type (Wright, 1977; Coleman & Prior, 1980). According to this mechanism, underflow currents carried sediment away from the point of discharge preventing the development of steep foresets (Gilbert type deltas) and leading to bed load deposition away from the shoreline (Farquharson, 1982). The described facies B successions favour comparisons with the mouth-bar type delta sequences documented by Farquharson (1982) from the Cretaceous of Antarctica. Similar lake deltas were also described from the Eocene Green River Formation of Utah (Ryder *et al.*, 1976), the Paleogene of Greenland (Pedersen, 1989) and present-day glacial lakes of Alaska and Massachusetts (Gustavson *et al.*, 1975).

Water depth calculations based on the thickness of asymmetric cycles were done following the method proposed by Klein (1974), also called the 'lake-filling model' by Gore (1988b). In lake settings, this method has been used among others by Van Dijk *et al.* (1978) and Farquharson (1982). In the present case, water depths of about 15 m are suggested for lake conditions recorded by assemblage 1. Problems of this and other methods to measure water depths have been discussed by Gore (1988b).

Preservation of thin parallel lamination in the fine-grained offshore sediments and absence of predepositional trace fossils suggest dysaerobic conditions. Postdepositional biogenic structures occur at the top of some mouth-bar sandstone beds, giving evidence of an improvement in the oxygen content related to the activity of river-induced currents.

On the other hand, the absence of terrigenous prograding sequences characterizes facies assemblage 2. According to relatively stable shorelines and absence of evaporites, deposition may have occurred in a hydrologically open lake. The existence of the event beds (facies D) records the action of episodic floods probably associated with seasonal rainfalls. The organic-rich shales (facies E, type II) offers important clues on environmental conditions.

Many perennial lakes show thermal or chemical stratification (e.g. Kelts & Hsü, 1978; Vincens *et al.*, 1986; Cohen, 1990). Near the surface, solar heating and atmospheric exchange result in warm oxygenated waters. Below the thermocline lies the deeper waters of the hypolimnion, cooler, denser and frequently anoxic.

Relatively thick organic-rich shale packages of the lower stratigraphic interval of facies assemblage 2 (Fig. 10; 35–71 m) suggest the existence of a permanent anoxic or near-anoxic water layer, probably reflecting incomplete turnovers of a stratified lake (meromictic lake). The absence of bioturbation, benthic organisms and current structures also supports this interpretation (Hentz, 1985; Allen & Collinson, 1986; Gore, 1988b, c). During the deposition of the black packages, lake depth probably reached a maximum. Towards the upper part of the lacustrine column, organic-rich shales virtually disappear. This change in facies pattern may evidence different water column conditions from those prevailing during the lower assemblage 2 stratigraphic interval (Fig. 10; 35–71 m). The arrangement of facies and the absence of thick organic-rich shale deposits suggest a progressively shallower lake affected by periodic recycling processes (*i.e.* holomixis), that precluded the accumulation and preservation of organic-rich sediments. Overturn events may have been controlled by the rainfall regime.

Lake evolution and climate control

Two types of lacustrine facies complexes have been recognized in the upper part of the Tanzhuang Formation. Facies assemblage 1 shows a clear dominance at the lower part of the section, whereas facies assemblage 2 becomes predominant towards the middle and upper part of the section (Fig. 10).

As previously mentioned, facies assemblage 1 is interpreted as formed in a shallow perennial lacustrine system under temperate permanently humid conditions. *Danaeopsis-Bernoulia* flora and the related microfloristic assemblage, dominated by pteridosperm and conifer pollen grains, support humid temperate conditions. During the time this facies complex was deposited, precipitation and freshwater inflow to the basin exceeded evaporation, infiltration and outflow (open conditions). The presence of a relatively diverse ostracode fauna (mainly darwinulids) within the fine-grained laminated sediments indicates permanent still shallow waters. The absence of evaporite crystals argues for low salinities. Perennial streams developed a deltaic system which generated the characteristic asymmetric cycles of facies assemblage 1.

In contrast, facies assemblage 2 is thought to reflect a significant change in lacustrine dynamics in direct relation to a climatic imprint. General features of this second lacustrine facies complex point to episodic flooding that resulted from periodic and probably strong seasonal precipitation, punctuated by relatively dry periods in a progressively shallower lake. Several lines of evidence support this hypothesis.

Sedimentologic evidence includes the presence of cyclic carbonate-clastic deposits (facies C) and flood event sandstones (facies D). The alternating carbonate-clastic couplets (facies C) were probably related to fluctuating relatively dry periods (low detrital influx) and wet periods (high detrital influx), controlled by seasonal precipitation and runoff to the lake. The ephemeral event deposits (facies D) represent episodic sheet floods that entered into a shallow lake (Fig. 13). These lacustrine deposits suggest an associated ephemeral drainage, controlled by episodic rainfall.

Additionally, the palynomorph assemblage and the nature of the organic matter also show distinct differences between both facies assemblages. Assemblage 2 microflora is dominated by the green algae *Botryoccocus*. This fact indicates predominance of endogenic organic matter and may suggest a significant autochthonous production. This well-known microflora is particularly abundant within the photic zone of undisturbed fresh to brackish waters in areas of relatively low rainfall (Guy-Olson, 1992). Extrabasinal organic matter mixed with clastic detritus tends to dilute the autochthonous organic input of the lacustrine biomass (Allen & Collinson, 1986). Accordingly, the abrupt increase in *Botryoccocus* content in the palynomorph assemblage may reflect the existence of long periods under relatively dry conditions with virtual absence of incoming terrigenous influx. Sheet floods entering into the lake during seasonal rainfalls could cause plankton mass-mortality, occasionally preserved under appropriate conditions (*i.e.* rapid settling, oxygen-depleted bottoms and high burial rate; cf. Katz, 1990; Talbot, 1988). In short, taking into account sedimentologic and paleontologic data, facies assemblage 2 seems to record a 'drier', pronounced seasonality climatic phase. This climatic signal may reflect either a global pattern (e.g. Pangaean monsoonal effect) or a local effect (e.g. altitude, orographic restrictions) (Olsen, 1990; Dubiel *et al.*, 1991).

The existence of periodic ephemeral runoff and general characteristics of event sandstone beds (facies D) suggest 'more arid' climatic conditions. However, evidences of true arid or semi-arid climate, such as caliche nodules, evaporite deposits and eolian sandstones (Gore, 1988b; Dubiel *et al.*, 1991) are apparently absent throughout the Tanzhuang lacustrine sequence.

Triassic paleogeographic reconstructions show that continents were assembled into a megacontinent, Pangaea (Fig. 14) (Hay *et al.*, 1982; Ziegler *et al.*, 1983; Parrish *et al.*, 1986). Unfortunately, the few paleomagnetic data available from China make eastern Pangaea reconstructions less reliable. However, it can be said with certainty that the fauna, flora and sedimentary facies associated indicate that the land mass was considerably further south than is indicated in most published reconstructions (Parrish *et al.*, 1986). Several studies give evidence of the important global paleoclimatic significance of the Pangaea supercontinent (Parrish *et al.*, 1986; Dubiel *et al.*, 1991; among many others). The symmetrical disposition of exposed land around the paleoequator maximized conditions for monsoonal circulation. Recently, some authors have called this paleoclimatic phenomenon the Pangaean megamonsoon (Dubiel *et al.*, 1991).

The term 'monsoon' refers to a peculiar climate system characterized by cross-equatorial flow, resulting from the thermal and pressure contrast between winter and summer hemispheres. The climatic signals of monsoon influence are (1) abundant seasonal rainfall, and (2) little annual temperature fluctuation (Dubiel *et al.*, 1991). According to studies of present-day monsoonal circulation in Asia, topographic highs represent heat sources that enhance precipitation in inland areas, favouring the development of the monsoonal system. Hahn & Manabe (1975) designed computer simulation models of Asia to evaluate topographic effects. Two models were compared: circulation patterns with mountains and with no-mountains. The comparison revealed that topography causes rainfall penetration farther into the continent interior, in desert-like areas predicted by the no-mountain model (Hahn & Manabe, 1975). Thus, it seems reasonable to consider the possible consequences of Pangaean topography. In particular, eastern Pangaea did contain large mountain ranges. A long mountain chain lay along the northern margin of the Tethys, comprising for example, the Palaeo-Tianshan and Palaeo-Qilian mountains (Fig. 5) (Wang, 1985). The presence of these mountain ranges must have had an important effect in Triassic paleoclimatic pattern.

If we analyze in some detail the early Mesozoic paleogeographic framework of China, we realize that several important tectonic events of Middle to Late Triassic times could have promotted a monsoonal influence in the Jiyuan-Yima area. The southern Yangtze platform (South China Block) was connected with the northern landmasses (North China Block) to form a single continent (Fig. 4). The Qinling region became an orographic chain as result of the Early Indosinian movements (Fig. 5). Additionally, the Tethys in the Qinghai-Xizang region experienced complex tectonic processes, resulting in the closure of the Songpan-Garze marginal sea trough (Fig. 5). These tectonic events led to the complete disappearance of the north-

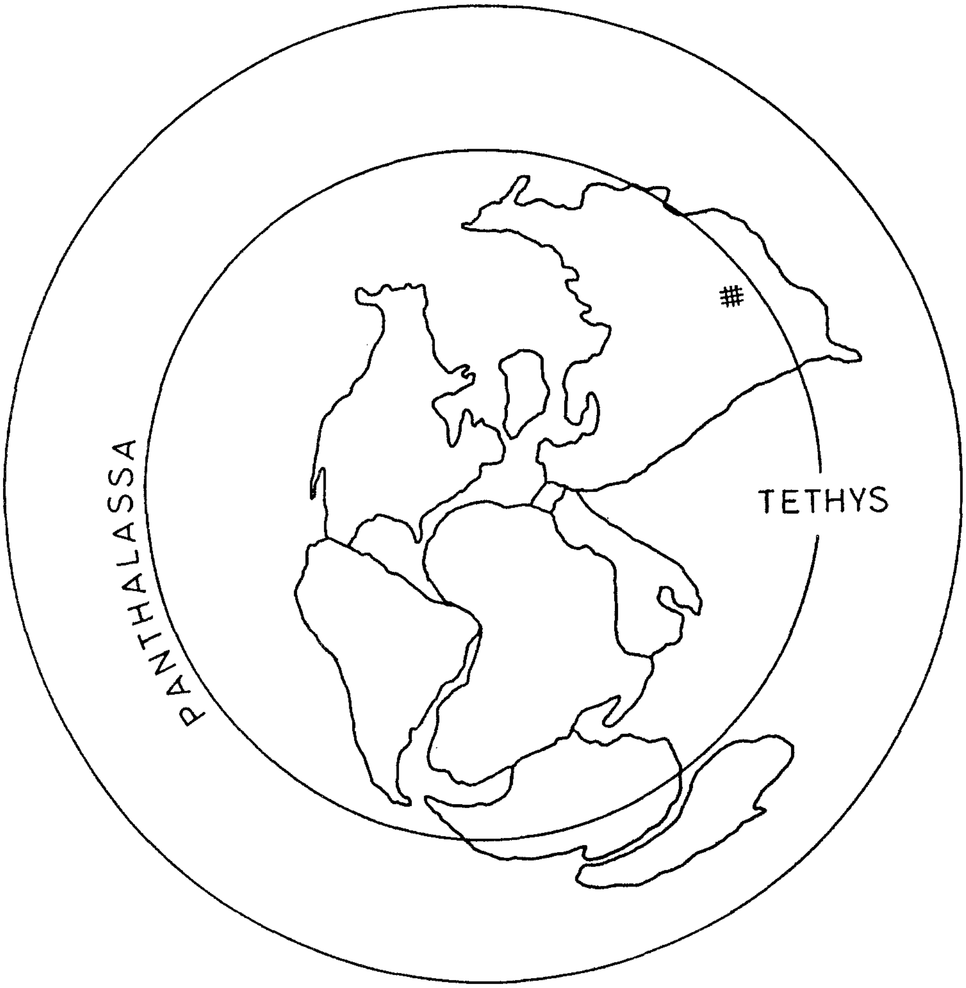

Fig. 14. Pangaea reconstruction during the Late Triassic (based on Veevers, 1991), showing the approximate location of the Jiyuan-Yima Basin. Lambert equal-area projection.

ern branch of the Tethys and the consequent growth of eastern Pangaea. The Tethys was restricted to the west to an area between the Himalaya region and the northern continental mass (Wang, 1985).

Towards the Late Triassic, most of the previously mentioned tectonic and paleogeographic changes have taken place. According to Chinese Late Triassic paleoclimatic reconstructions, the Jiyuan-Yima area was located at the southern margin of the Ordos Megabasin within a humid temperate climatic belt. This area was located close to the tropical-subtropical climatic zone (Wang, 1985). As a working hypothesis, strong seasonality evidenced towards the middle and upper part of the Tanzhuang lake column may reflect the influence of Pangaean magamonsoon circulation system. Further research is encouraged in order to test this paleoclimatic hypothesis.

Acknowledgments

We would like to thank the Chinese Academy of Sciences and the Third World Academy of Sciences (TWAS), who supported the research visit to China of MGM and LAB. The visitant authors particularly wish to remark the politeness and efficiency of the Foreign Affairs Office Staff of the Jiaozuo University and the hospitality of the people of Jiaozuo. We also would like to express our gratitude to Guillermo Ottone who supplied all the palynologic data, Wu Linyouling for the ostracode information, and Hector Villar who provided the organic geochemistry analysis. The final manuscript benefited from the comments of reviewers Pamela Gore and Dale Leckie. Illustrations were kindly made by Guillermo Guirado whose help is greatly acknowledged.

References

Allen, P. A. & J. D. Collinson, 1986. Lakes. In H. G. Reading (ed.), Sedimentary environments and facies. Blackwell Scientific Publications, Oxford: 63–94.

Bates, C. C., 1953. Rational theory of delta formation. American Association of Petroleum Geologists, Bulletin 37: 2119–2162.

Buatois, L. A., M. G. Mángano, X. Wu & G. Zhang, in review. Jurassic lake deposits from the Anyao Formation, central China. In E. Gierlowski-Kordesch & K. Kelts (ed.), Global Geological Record of Lake Basins. Cambridge University Press, Cambridge.

Cohen, A. S., 1990. Tectono-stratigraphic model for sedimentation in Lake Tanganyka, Africa. In B. J. Katz (ed.), Lacustrine basin exploration. Case studies and modern analogues. American Association of Petroleum Geologists, Memoir 50: 137–150.

Coleman, J. M & D. B. Prior, 1980. Deltaic Sand Bodies. American Association of Petroleum Geologists Short Course Note Series 15, 171 pp.

Dubiel, R. F., J. T. Parrish, M. Parrish & S. C. Good, 1991. The Pangaean megamonsoon – Evidence from the Upper Triassic Chinle Formation, Colorado Plateau Palaios 6: 347–370.

Farquharson, G. W., 1982. Lacustrine deltas in a Mesozoic alluvial sequence from Camp Hill, Antarctica. Sedimentology 29: 717–725.

Gilbert, R., 1975. Sedimentation in Lilloet Lake, British Columbia. Can. J. Earth Sci. 12: 1697–1711.

Gore, P. J. W., 1988a. Paleoecology and sedimentology of a Late Triassic lake, Culpeper Basin, Virginia, USA. Palaeogeog., Palaeoclim., Palaeoecol. 62: 593–608.

Gore, P. J. W., 1988b. Lacustrine sequences in an early Mesozoic rift basin: Culpeper Basin, Virginia, USA. In A. J. Fleet, K. Kelts & M. R. Talbot (eds.), Lacustrine Petroleum Source Rocks. Geological Society Special Publication 40: 247–278.

Gore, P. J. W., 1988c. Late Triassic and Early Jurassic lacustrine sedimentation in the Culpeper basin Virginia. In W. Manspeizer (ed.), Triassic Jurassic Rifting. Continental breakup and the origin of the Atlantic Ocean and passive margins. Part A Elsevier, Amsterdam: 369–400.

Gore, P. J. W., 1989. Toward a model for open- and closed-basin deposition in ancient lacustrine sequences: the Newark Supergroup (Triassic-Jurassic), Eastern North America. Palaeogeog., Palaeoclim., Palaeoecol. 70: 29–51.

Gustavson, T. C., G. M. Ashley & J. C. Boothroyd, 1975. Depositional sequences in glaciolacustrine deltas. In A. V. Jopling & B. C. McDonald (eds.), Glaciofluvial and glaciolacustrine sedimentation. Society of Economic Paleontologists and Mineralogists Special Publication 23: 264–280.

Guy-Ohlson, D., 1992. *Botryococcus* as an aid in the interpretation of palaeoenvironment and depositional processes. Rev. Paleobot. Palynol. 71: 1–15.

Hahn, D. G. & S. Manabe, 1975. The role of mountains in the South Asia monsoon circulation. J. Atmosph. Sci. 32: 1515–1541.

Hay, W. W., J. F. Behensky, E. J. Barron & J. L. Sloan, 1982. Late Triassic-Liassic paleoclimatology of the proto-central North Atlantic rift system. Palaeogeog., Palaeoclimatol., Palaeoecol. 40: 13–30.

Hentz, T. F., 1985. Early Jurassic sedimentation of a rift-valley lake: Culpeper basin, northern Virginia. Geological Society of America, Bulletin 96: 92–107.

Hsü, K. J., 1989. Origin of sedimentary basins of China. In X. Zhu (ed.), Chinese Sedimentary Basins. Elsevier, Amsterdam: 207–227.

Hu, B., 1991. On the Late Triassic-Middle Jurassic continental stratigraphy from Jiyuan, western Henan Province. J. Stratigr. 15: 48–52. (In Chinese with English summary).

Kang, M., F. Meng, B. Ren & B. Hu, 1984. The age of Yima Formation and the establishment of the Yangshuzhuang Formation. J. Stratigr. 8. (In Chinese with English summary).

Kang, M., F. Meng, B. Ren, B. Hu & Z. Ching, 1985. Division and correlation of the Mesozoic coal-bearing stratigraphy from Henan Province. Journal of Jiaozuo Mining Institute 5. (In Chinese with English summary).

Katz, B. J., 1990. Controls on distribution of lacustrine source rocks through time and space. In B. J. Katz (ed.), Lacustrine basin exploration. Case studies and modern analogues. Am. Ass. Petrol. Geolog. 50: 61–76.

Kelts, K., 1988. Environments of deposition of lacustrine petroleum source rocks: an introduction. In A. J. Fleet, K. Kelts & M. R. Talbot (eds.), Lacustrine Petroleum Source Rocks. Geological Society Special Publication 40: 3–27.

Kelts, K. & K. Hsü, 1978. Freshwater carbonate sediments. In A. Lerman (ed.), Lakes: Chemistry, geology and physics. Springer-Verlag, New York: 295–323.

Klein, G. D., 1974. Estimating water depths from analysis of barrier island and deltaic sedimentary sequences. Geology 21: 409–412.

Li, D. & M. Luo, 1990. Hydrocarbon accumulation in Mesocenozoic lacustrine remnant petroliferous depressions and basins, southeastern China. In B. J. Katz (ed.), Lacustrine basin exploration. Case studies and modern analogues. American Association of Petroleum Geologists Memoir 50: 327–333.

Lin, C., Q. Yang & S. Li, 1991. Structural and depositional patterns of the Tertiary Baise Basin, Guang Xi Autonomous Region (southeastern China): a predictive model for fossil fuel exploration. In P. Anadón, Ll. Cabrera & K. Kelts (eds.), Lacustrine facies analysis. International Association of Sedimentologists Special Publication 13: 75–92.

Mángano, M. G., L. A. Buatois, X. Wu, J. Sun & G. Zhang, in review. Triassic lacustrine sedimentation from the Tanzhuang Formation, Jiyuan-Yima Basin, southeastern China. In E. Gierlowski-Kordesch & K. Kelts (eds), Global Geological Record of Lake Basins. Cambridge University Press, Cambridge.

Olsen, P. E., 1990. Tectonic, climatic, and biotic modulation of lacustrine ecosystems – Examples from Newark Supergroup of Eastern North America. In B. J. Katz (ed.), Lacustrine basin exploration. Case studies and modern analogues. American Association of Petroleum Geologists Memoir 50: 209–224.

Parrish, J. M., J. T. Parrish & A. M. Ziegler, 1986. Permian-Triassic paleogeography and paleoclimatology and implications for therapsid distributions. In N. H. Hotton III, P. D. MacLean, J. J. Roth & E. C. Roth (eds.), The biology of mammal-like reptiles. Smithsonian Press, Washington, D.C.: 109–132.

Pedersen, G. K., 1989. A fluvial-dominated lacustrine delta in a volcanic province, W Greenland. In M. K. G. Whateley & K. T. Pickering (eds.), Deltas: Sites and traps for fossil fuels. Geological Society Special Publication 41: 139–146.

Platt, N. H. & V. P. Wright, 1991. Lacustrine carbonates: facies models, facies distributions and hydrocarbon aspects. In P. Anadón, Ll. Cabrera & K. Kelts (eds.), Lacustrine facies analysis. International Association of Sedimentologists Special Publication 13: 57–74.

Ryder, R. T., T. D. Fouch & J. H. Elison, 1976. Early Tertiary sedimentation in western Uinta Basin, Utah. Geological Society of America, Bulletin 87: 496–512.

Seilacher, A., 1991. Events and their signatures. An overview. In G. Einsele, W. Ricken & A. Seilacher (eds.), Cycles and events in stratigraphy. Springer-Verlag, Berlin: 222–227.

Sen, D. P. & T. Banerji, 1991. Permo-Carboniferous proglacial-lake sedimentation in the Sahajuri gondwana basin, India. Sed. Geol. 71: 47–58.

Shaw, J., 1975. Sedimentary successions in Pleistocene ice- marginal lakes. In A. V. Jopling & B. C. McDonald (eds.), Glaciofluvial and glaciolacustrine sedimentation. Society of Economic Paleontologists and Mineralogists Special Publication 23: 281–303.

Stanley, K. O. & R. C. Surdam, 1978. Sedimentation on the front of Eocene Gilbert-type deltas, Washakie Basin, Wyoming. J. Sed. Petrol. 48: 557–573.

Steiner, M., J. Ogg, Z. Zhang & S. Sun, 1989. The Late Permian/Early Triassic magnetic polarity time scale and plate motions of South China. J. Geophys. Res. 94: 7343–7363.

Sturm, M. & A. Matter, 1978. Turbidites and varves in Lake Brienz (Switzerland): deposition of clastic detritus by density currents. In A. Matter & M. E. Tucker (eds.), Modern and Ancient Lake Sediments. International Association of Sedimentologists Special Publication 2: 147–168.

Sun, J., 1992. Lacustrine sedimentary features and oil and gas reservoir potential of the Tanzhuang Formation in Jiyuan, western Henan. Mater Deggree Dissertation, Jiaozuo Mining Institute. Unpublished, 111 pp.

Talbot, M. R., 1988. The origin of lacustrine oil source rocks: evidence from the lakes of tropical Africa. In A. J. Fleet, K. Kelts & M. R. Talbot (eds.), Lacustrine Petroleum Source Rocks. Geological Society Special Publication 40: 29–43.

Van Dijk, D. E., D. K. Hobday & A. J. Tankard, 1978. Permo-Triassic lacustrine deposits in the Eastern Karoo Basin, Natal, South Africa. In A. Matter & M. E. Tucker (eds.), Modern and Ancient Lake Sediments. International Association of Sedimentologists Special Publication 2: 225–239.

Veevers, J. J., 1991. Mid-Triassic lacuna on the Gondwanaland platform during the final coalescence and incipient dispersal of Pangaea. In H. Ulbrich & A. C. Rocha Campos (eds.), Gondwana Seven Proceedings Seventh International Gondwana Symposium. Sao Paulo: 201–216.

Vincens, A., J. Casanova & J. J. Tiercelin, 1986. Palaeolimnology of Lake Bogoria (Kenya) during the 4500 BP high lacustrine phase. In L. E. Frostick, R. W. Renaut, I. Reid & J. J. Tiercelin (eds), Sedimentation in the African Rifts. Geological Society Special Publication 25: 323–330.

Wang H., comp., 1985. Atlas of the Palaeogeography of China. Cartographic Publishing House, Beijing, 283 pp.

Wright, L. D., 1977. Sediment transport and deposition at river mouths: a synthesis. Geological Society of America, Bulletin 88: 857–868.

Wu, X., 1985. Trace fossils from lake turbidites of the Jiyuan-Yima Basin, western Henan Province. Acta Sedimentologica Sinica 3: 23–31.

Zhou, Z. & P. Li, 1980. Discussion on the division, correlation and age of the Mesozoic continental stratigraphy of China based on plant fossils. Geological Symposium for International Exchange 4, Stratigraphy and Paleontology, Geological Publishing House, Beijing.

Zhu, X., 1989. Chinese Sedimentary Basins. Elsevier, Amsterdam, 238 pp.

Ziegler, A. M., C. R. Scotese & S. F. Barrett, 1983. Mesozoic and Cenozoic paleogeographic maps. In P. Broschie & J. Sundermann (eds.), Tidal friction and the earth's rotation. II. Springer-Verlag, Berlin: 240–252.